

General Disclaimer

One or more of the Following Statements may affect this Document

- This document has been reproduced from the best copy furnished by the organizational source. It is being released in the interest of making available as much information as possible.
- This document may contain data, which exceeds the sheet parameters. It was furnished in this condition by the organizational source and is the best copy available.
- This document may contain tone-on-tone or color graphs, charts and/or pictures, which have been reproduced in black and white.
- This document is paginated as submitted by the original source.
- Portions of this document are not fully legible due to the historical nature of some of the material. However, it is the best reproduction available from the original submission.

NASA CR-175253

(NASA-CR-175253) DEVELOPMENT OF LONG
WAVELENGTH SEMICONDUCTOR DIODE LASERS NEAR
28 MICRONS FOR USE IN INFRARED HETERODYNE
SPECTROMETERS Final Report (Laser
Analytics, Inc., Bedford, Mass.) 60 p

N84-32802

Unclass
22265

G3/36

 **Spectra-Physics**



Laser Analytics Division

25 Wiggins Avenue, Bedford, MA 01730, Tel. (617) 275-2650

FINAL REPORT
DEVELOPMENT OF LONG WAVELENGTH
SEMICONDUCTOR DIODE LASERS NEAR
28 μm FOR USE IN INFRARED
HETERODYNE SPECTROMETERS

Contract NAS5-26200
Amendment No. 6

June, 1984

National Aeronautics and Space Administration
Goddard Space Flight Center
Greenbelt Road
Greenbelt, MD 20771

By

Kurt J. Linden ✓
Laser Analytics, Inc.
25 Wiggins Avenue
Bedford, Massachusetts 01730

TABLE OF CONTENTS

1.0 INTRODUCTION

2.0 CRYSTAL GROWTH AND JUNCTION FORMATION

- 2.1 Preparation of Growth Ingots
- 2.2 Crystal Growth and Characterization
- 2.3 Carrier Concentration Studies
- 2.4 Junction Formation

3.0 WAFER PROCESSING AND LASER FABRICATION

- 3.1 Striping
- 3.2 Laser Fabrication
- 3.3 Surface Treatment Investigation

4.0 LASER EVALUATION AND RESULTS

- 4.1 Regular-cavity Lasers
- 4.2 Narrow-stripe Lasers
- 4.3 Short-cavity Laser with Narrow Stripes

5.0 RETEST OF PREVIOUSLY FABRICATED LASERS

6.0 DELIVERABLE LASERS

7.0 SUMMARY AND CONCLUSION

8.0 RECOMMENDATIONS FOR FUTURE WORK

9.0 REFERENCES

APPENDIX

Publications and Talks during Contract Period

LIST OF TABLES

1. Summary of some properties of the ten crystals grown during the contract period.
2. Effect of isothermal annealing on carrier concentration and laser emission frequency.
3. Historical data used in an attempt to correlate starting frequency with material parameters.
4. List of 3 vacuum baked lasers showing their contact resistance (R_f) and threshold current (I_{th}) values both before and after a 16 hour, 95°C vacuum bake.
5. List of lasers assembled during the contract period. All lasers are mesa-stripe structures. RC = regular cavity, NS = narrow stripe and SC = short cavity configuration.
6. Summary of physical, electrical and optical characteristics of three regular cavity (RC) mesa-stripe lasers fabricated during the early part of the program.
7. Comparison of performance of narrow mesa-striped (20 μ m) lasers with different cavity length.
8. Optical retest data for lasers fabricated during the past four years on contract NAS5-26200.
9. List of lasers fabricated during the contract period and some of their performance parameters.
10. Comparison of contract goals and actual achievements during the contract period.

LIST OF FIGURE CAPTIONS

1. SEM micrographs of a 28 μm diode laser with a 20 μm mesa width. Top portion shows SE + EBIC photograph and bottom shows just the EBIC photograph.
2. Emission spectra of laser 3349-28 at 15K and at 2 different values of laser current: 0.15A and 0.5A
3. Emission spectrum of laser 3349-28 at 15K and 1A. Total power at 1A is 320 μW .
4. Family of emission spectra from laser 3350-02 at 15K showing evolution of spectral modes with increasing laser current. Output at various current values is shown in parentheses.
5. Emission spectra of laser 3350-17 at 15K.
6. Emission spectra of laser 3350-17 at 25K. Longitudinal mode separation is 3.5 cm^{-1} .
7. Emission spectra of laser 4079-13 at 15K and 39K.
8. Emission spectra of laser 4090-19 at low temperatures.
9. Emission spectra of laser 4079-13 at various current levels, illustrating evolution of the emission spectrum with increasing current. $T=15\text{K}$.
10. Emission spectra of laser 4094-01 at 25K and 13 different current values, showing single mode emission below 350 mA.
11. Emission spectra of laser 4094-07 at various current levels and at 20K. Power output at 1A is 323 μW and maximum CW operating temperature is 42K at 1A.

12. Detailed emission spectrum of laser 4094-07 at 20K near threshold.
The laser emitted single mode at approximately 30.2 μm and was tunable over approximately 1.0 cm^{-1} .
13. Optical retest data for laser NLW-1 at 15K and 1 Amp.
14. Optical retest data for laser NLW-1 at 15K and 2 Amps.
15. Optical retest data for laser NLW-3 at 15K, 2 Amps.
16. Optical retest data for laser 2032-25 at 15K, 1 Amp.
17. Optical retest data for laser 2032-25 at 15K, 2 Amps.
18. Optical retest data for laser 2084-42 at 15K, 2 Amps.
19. Optical retest data for laser 2084-52 at 15K, 0.90 Amps.
20. Optical retest data for laser 2127-06 at 15K, 1.9 Amps.
21. Optical retest data for laser 2127-51 at 27K, 1.9 Amps.
22. Optical retest data for laser 2127-51 at 15K, 1.88 Amps.
23. Optical retest data for laser 2132-56 at 15K, 2.0 Amps.
24. Optical retest data for laser 3088-04 at 15K, 2.0 Amps.
25. Optical retest data for laser 3088-04 at 15K, 1.0 Amps.

Foreword

This final report covers the period from June, 1983 through June, 1984, corresponding to amendment six of contract NAS5-26200. The technical monitor for this contract was Dr. Theodor Kostluk.

The goals and objectives of this contract have been met with the development of short cavity, narrow stripe lasers exhibiting improved spectral characteristics and, in some cases, single mode emission in the 28.2 μm spectral region. Such improved lasers are required for use in infrared heterodyne spectrometers utilizing long wavelength, high speed HgCdTe photodiode detectors being simultaneously developed at the MIT Lincoln Laboratory.

1.0 INTRODUCTION

This report describes the work carried out and the results achieved on a one-year effort aimed at developing tunable diode lasers operating in the 28 μm spectral region for use in infrared heterodyne spectrometers. The goals of the contract have been achieved with the successful development of a process capable of yielding lasers emitting 500 μW of multimode power, 112 μW in a true single mode and true single-mode operation at laser currents of up to 35% above threshold. These results, which are considerably better than the program goals, were obtained from narrow mesa-stripe (20 μm wide) short cavity (120 μm length) laser configurations. Six stripe-geometry lasers, with a variety of cavity widths and lengths were delivered to Dr. David Spears at the MIT Lincoln Laboratory for evaluation.

During this contract period we have obtained control of the techniques needed to fabricate such devices. In addition to this success, we have demonstrated the long-term reliability of such lasers by having obtained reproducible electrical and optical output characteristics from lasers fabricated during earlier phases of the program, going back to 3-year old devices.

2.0 CRYSTAL GROWTH AND JUNCTION FORMATION

2.1 Preparation of Growth Ingots

Crystals were grown from purified ingots of $\text{Pb}_{0.9}\text{Sn}_{0.1}\text{Se}$ which were obtained by reacting stoichiometric quantities of the binary compounds PbSe and SnSe . Flame spectroscopy analysis of representative ingots typically showed impurity concentrations of a few ppm. Ingots obtained in this manner were then loaded into quartz ampoules for growth of $\text{Pb}_{0.9}\text{Sn}_{0.1}\text{Se}$ single crystals.

2.2 Crystal Growth and Characterization

As during previous phases of the program, crystals were grown from the above described ingots by the closed-tube sublimation technique.¹ The reacted ingots were crushed and loaded into growth ampoules, placed on vacuum pumps, evacuated and sealed. The growth ampoules were placed into profiled, horizontal growth furnaces and the closed-tube, sublimation growth was carried out at approximately 800°C . The resulting crystals typically consisted of (100)-oriented facets of high quality which were characterized by etch-pit density counts of approximately 10^3 cm^{-2} . Carrier concentrations were determined by measuring thermal probe voltages and using previously obtained Hall-data which provided a correlation between thermal probe voltage and carrier concentration. Such thermal probe measurements are considerably faster to make and entail less risk of sample damage than Hall measurements.

A summary of the data obtained for the ten as-grown crystals obtained during the contract period is shown in Table 1. In a previous final report (dated June, 1983), we had reported that attempts to obtain reproducible carrier concentrations by isothermal annealing of the grown crystals were successful, but resulted in unacceptably high carrier concentrations ($2\text{--}4 \times 10^{19} \text{ cm}^{-3}$). Such high carrier concentrations (considerably higher than those observed in as-grown crystals) were suspected of being responsible for yielding lasers which emitted at wavelengths considerably

Crystal No.	Approximate Size (mm)	Probe Voltage (mV)	Carrier Concentration (cm ⁻³)
2257	4 x 4	18	8×10^{18}
2279	3 x 4	25	3×10^{18}
2281	5 x 5	20	7×10^{18}
2282	3 x 5	23	5×10^{18}
2285	4 x 6	23	5×10^{18}
2290	4 x 4	15	1.5×10^{19}
2295	5 x 5	16	1.4×10^{19}
2321	4 x 6	13	1.6×10^{19}
2356	4 x 7	19	6.5×10^{18}
2367	3 x 4	14	1.55×10^{19}

TABLE 1

Summary of some properties of the ten crystals grown during the contract period

shorter than expected for material of composition $\text{Pb}_{0.9}\text{Sn}_{0.1}\text{Se}$. This effect is described in more detail in the next section.

2.3 Carrier Concentration Studies

Work carried out during the early part of this contract period confirmed the above noted suspicion that crystals with high carrier concentration (above approximately $2 \times 10^{19} \text{ cm}^{-3}$) yield lasers that can emit at energies greater than that expected from the band gap of the material. For example, it was found that two wafers processed in this manner (i.e., the material was isothermally annealed in a chalcogen-rich atmosphere to fix the carrier concentration in the $2\text{--}3 \times 10^{19} \text{ cm}^{-3}$ range) each yielded lasers which emitted at frequencies higher than expected for this composition value. Since this phenomenon was generally not observed for unannealed material (unless such unannealed material had carrier concentrations of $2\text{--}3 \times 10^{19} \text{ cm}^{-3}$ or higher), it is thought to be caused by the Burstein effect.² A Burstein shift is known to occur for small-bandgap materials which are heavily doped, and is due to an effective increase in the semiconductor band gap due to band-filling resulting from the high carrier concentration. The effect is best seen by examining the data shown in Table 2, which illustrates that isothermal annealing, while yielding reproducible carrier concentrations, causes these carrier concentrations to be so large as to induce a Burstein shift of from 50 to 100 cm^{-1} in finished lasers. In both of the crystals of Table 2, a chalcogen-rich $\text{Pb}_{0.9}\text{Sn}_{0.1}\text{Se}$ annealing source was used to insure that any laser emission frequency shift would not be caused by crystal compositional changes that could occur if the anneals were carried out with PbSe sources.

2.4 Junction Formation

Pn junctions were obtained in both the annealed and unannealed wafers by diffusion from undoped, metal-rich PbSe, or $\text{Pb}_{0.9}\text{Sn}_{0.1}\text{Se}$ sources. To avoid surface composition changes which could arise from the use of PbSe diffusion sources, the first experiments on diffusing annealed material used

Wafer No.	Post Anneal Probe Voltage	Carrier Concentration (cm ⁻³)	Laser Frequency (cm ⁻¹)
4504	10	2.8×10^{19}	382
4642	11	2.7×10^{19}	458

TABLE 2

Effect of isothermal annealing on carrier concentration and laser
emission frequency.

a metal-rich $\text{Pb}_{0.9}\text{Sn}_{0.1}\text{Se}$ source. The 700°C diffusions were carried out on the annealed material described in Table 2. The resulting laser emission frequencies, as noted in the previous section, were too high. Since a $\text{Pb}_{0.9}\text{Sn}_{0.1}\text{Se}$ diffusion source was used, the possibility of the wavelength shift being due to compositional changes at the wafer surface is precluded because the diffusion source composition is identical to the crystal composition. It was therefore concluded that the emission wavelength shift was, in fact, a Burstein shift. Based on this evidence only PbSe diffusion sources were used. No diffusion sources with intermediate x-values ($\text{Pb}_{1-x}\text{Sn}_x\text{Se}$ with $0 < x < .1$) were used because no purpose would be served once it was proven that surface composition changes were not responsible for the emission wavelength shift.

Results during the previous contract year had indicated that some lasers fabricated from converted material did not exhibit the above-noted Burstein shift. A correlation study was therefore carried out to determine the degree of reproducibility of obtaining 350 cm^{-1} emission from annealed material diffused at a variety of temperatures. Results from a total of 20 diffusions were analyzed. The data are summarized in Table 3. The numbers under C# correspond to the anneal runs, while the numbers under D# column correspond to the junction diffusion run. Of the 20 diffusions, only 6 yielded devices which emitted below 350 cm^{-1} . Five of these had deep junctions (which are difficult to mesa-stripe) and only one had a shallow ($2\text{ }\mu\text{m}$) junction. It is therefore clear that diffusion of p-converted wafers is not a reproducible method of obtaining $28.2\text{ }\mu\text{m}$ lasers. The reason appears to be connected with the occurrence of a Burstein shift for most of the wafers. In those cases where a deeper junction occurred, less of a shift was observed, possibly because deeper junctions are more graded and therefore may have a somewhat lower carrier concentration near the junction region.

D#	T/t	j Depth (μm)	C#	C Probe	Start Freq. (cm^{-1})
4642	700/1	15	4633	+11	458
4504	700/1	7	4459	+10	382
4319	700/2	3	4275	+10	415
4317	700/2	2	4272	+11	407
4316	700/2	2	4273	+11	347
4315	700/2	2	4298	+9	358
4314	700/2	2	4298	+9	390
4313	700/2	3	4297	+9	377
4312	700/1	4	4296	+10	405
4219	650/24	2	4136	+12	493
4145	650/24	20	4132	+11	411
3654	700/8		3072	+13	361
3653	700/8	38	3070	+10	346
3652	700/4		3168	+15	450
3381	700/2	56	3125	+11	332
3309	675/1/2	7	3254	+13	372
3246	650/24	19	3169	+11	336
3245	700/16	50	3167	+11	345
3211	700/1/2		3129	+10	391
3134	700/2	13	3069	+10	330

TABLE 3

Historical data used in an attempt to correlate starting frequency with material parameters.

3.0 WAFER PROCESSING AND LASER FABRICATION

3.1 Striping

During the previous year the technology of fabricating mesa-stripe lasers was extended to include material in the 28.2 μm spectral region. At that time relatively wide (approximately 50 to 100 μm) mesas were used. The technology was further refined during the first portion of the present effort, and during the latter portion it was demonstrated that long wavelength lasers could be made with stripe widths as narrow as 20 μm (only about 3 times as wide as the wavelength of the laser radiation in the laser crystal). Two photographs of such a narrow-stripe, long wavelength laser are shown in Figure 1. Both were taken with a scanning electron microscope (SEM). The top photograph of the laser face was taken in the normal secondary emission (SE) mode, with a second exposure showing only the electron-beam-induced current (EBIC) response superimposed. Thus this top photograph shows both SE image of the mesa-portion of the laser face (which was cleaved) and the superimposed EBIC image. From the brightness of the EBIC image it can be seen that this laser has a junction depth of a few μm (as previously verified by thermal probing an angle-lapped cross section of a different portion of the same diffused wafer). The light portion just under the electrical contact region extends over a distance of approximately 3 to 5 μm below the mesa surface, and represents that region of the laser face that is expected to emit the laser radiation. Since the light EBIC region is difficult to see, a separate photograph showing only the EBIC signal is shown in the lower photograph of Figure 1. Here again, it is apparent that the laser wafer has a junction depth of approximately 3 to 5 μm and a mesa stripe width of approximately 20 μm . It was necessary to cool the laser to liquid nitrogen temperature while taking the EBIC photographs in the SEM analysis. This is generally not necessary for shorter wavelength ($< 20 \mu\text{m}$) lasers, but appears to be necessary for long wavelength lasers.³

ORIGINAL
OF POOR QUALITY

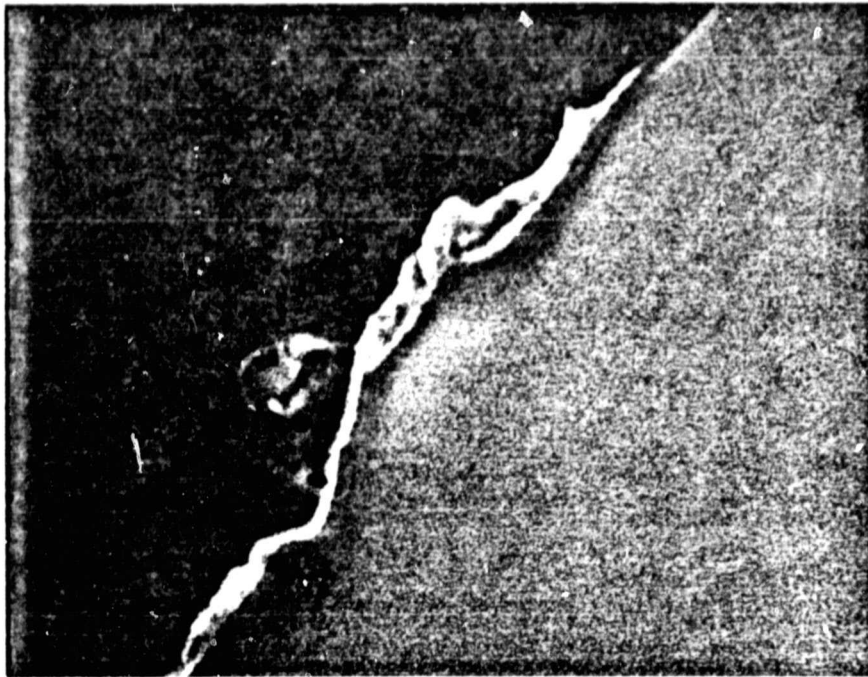


Figure 1

SEM micrographs of a 28 μm diode laser with a 20 μm mesa width. Top portion shows SE + EBIC photograph and bottom shows just the EBIC photograph.

3.2 Laser Fabrication

The lasers fabricated during this program were assembled by standard Laser Analytics procedures as described in an earlier report. The lasers assembled during the contract period fall into 3 categories:

1. Regular cavity stripe lasers (RC)
2. Narrow stripe lasers (NS)
3. Short cavity lasers (SC)

We have found that the narrow stripe (NS) lasers and, in particular, the short cavity (SC) narrow stripe lasers yielded the best device performance in terms of being able to obtain single mode operation. We describe the performance of the various laser types in Section 4.0. The mounting of the short cavity laser dice presented a particular problem due to the geometric structure of these devices. On the one hand, the laser die must be mounted as close to the front of the laser stud as possible, but on the other hand, the die must not hang over the end. It is often difficult to even make the laser die stand on the stud at all. Special handling methods were used.

3.3 Surface Treatment Investigation

One of the parameters responsible for the slight variations in laser operating characteristics which sometimes occur between test runs is the existence of a shunt leakage current. Small changes in leakage current are expected to occur because neither the mesa edges nor the laser end facets are truly passivated. Thus any slight oxide formation, moisture interaction or interaction with other atmospheric ambients, could cause changes in shunt leakage current. Passivating agents have been developed for a number of common semiconductor materials, but even with a material as well developed as silicon, passivation problems still exist if such devices are not hermetically sealed.

Past experiments in this laboratory have shown that it is possible to obtain reductions in the shunt leakage current of 5 μm and 10 μm lasers by vacuum baking such devices at approximately 90°C overnight. Such experiments had never been carried out for long wavelength diode lasers, however, and we report here on the results of the first experiment of this type carried out on diode lasers made from $\text{Pb}_{0.9}\text{Sn}_{0.1}\text{Se}$ in the mesa stripe configuration. The lasers evaluated were chosen from among those fabricated and tested during the year preceeding this program. Thus considerable stability data are available for each of these lasers. Furthermore, only lasers whose starting frequency was slightly higher than desired were studied, so as not to jeopardize any lasers useful for 28.2 μm heterodyne work.

A list of the 2 lasers investigated, as well as a history of their contact resistance and threshold current values both before and after the vacuum baking experiment is shown in Table 4. In neither case there was a significant change in threshold current, speaking well for the relative passivative quality of the insulating layer covering the mesa edges. The abrupt contact resistance decrease of laser 3085-18 to its original value indicates some abnormal behavior between the initial and the post-bake test. Such resistance increases are not typical in these lasers and could, in this case, indicate a solder lead instability.

Laser No.	Test Date	R_f (mohm)	I_{th} (mA)	Comments
3085-10	3-28-83	8	514	
	6-15-83	8	486	
	9-23-83	8	470	
	12-21-83	8	490	
	3-15-84	8	481	
	6-13-84	8	475	95°C/16H vac. bake
3085-18	3-28-83	15	200	
	6-15-83	32	171	
	9-23-83	29	175	
	12-21-83	29	180	
	6-18-84	17	183	95°C/16H vac. bake

TABLE 4

List of 2 vacuum baked lasers showing their contact resistance, R_f , and threshold current, I_{th} , both before and after a 16 hour 95°C vacuum bake.

4.0 LASER EVALUATION AND RESULTS

4.1 Regular Cavity Lasers

During this program we have demonstrated that striped lasers of $\text{Pb}_{0.9}\text{Sn}_{0.1}\text{Se}$ emitting in the $28.2\text{ }\mu\text{m}$ spectral region can be reproducibly achieved. These lasers were of the mesa-stripe configuration, with mesa heights of from 5 to approximately $20\text{ }\mu\text{m}$, depending on junction depth. It was demonstrated that by using as-grown, p-type crystals, without any annealing procedure, the Burstein shift previously observed with annealed material could generally be avoided. The junction depth variations observed with various wafers is thought to be due to variations in the carrier concentrations of the as-grown crystals. Such as-grown concentrations were found to be typically in the $5\text{--}6 \times 10^{18}\text{ cm}^{-3}$ range, with the exact value difficult to control. This lack of control, however, was found not to be a serious problem because the spread was generally narrow enough to ensure diffused junction depths within a range that can easily be handled with standard photolithographic techniques. The option of rejecting wafers with excessive junction depths (i.e., $> 20\text{ }\mu\text{m}$) also presents no problems since such wafers are rare and can be identified at a stage where only a minimal processing effort has been invested.

Regular cavity length lasers, with stripe lengths of $210\text{ }\mu\text{m}$ were fabricated from 3 different wafers, with mesa widths ranging from 50 to $85\text{ }\mu\text{m}$. These lasers are shown as the top three entries of Table 5. While these cavity dimensions were known not to be optimal, they represent a significant advantage over the previously studied broad-area lasers in that the mesa stripe configuration precludes the existence of internally reflecting modes and sideways-emitting modes. The physical, electrical and characteristics of the three regular cavity lasers are summarized in Table 6. As is typical of this long wavelength, narrow gap material, the contact resistance is low (< 14 milliohms). Each of the lasers emits more than the program goal of $20\text{ }\mu\text{W}/\text{mode}$. In fact, each emits more than twice this value, one emitting four times as much power per mode at $28\text{ }\mu\text{m}$. The far-field emission patterns were measured for each of the lasers with a pyroelectric detector of 1 cm^2

Laser No.	D No.	Cavity Dimensions	Category
3349-28	4772	W = 85 μ m L = 210 μ m	RC
3350-02	4673	W = 50 μ m L = 210 μ m	RC
3350-17	4768	W = 50 μ m L = 210 μ m	RC
4079-13	4864	W = 20 μ m L = 250 μ m	NS
4090-19	4946	W = 20 μ m L = 250 μ m	NS
4094-01	4944	W = 20 μ m L = 120 μ m	SC
4094-07	4946	W = 20 μ m L = 120 μ m	SC

TABLE 5

List of lasers assembled during the contract period. All lasers are mesa-stripe structures. RC = regular cavity, NS = narrow stripe and SC = short cavity configuration.

Laser No.	3349-28	3350-02	3350-17
Wafer No.	S4772	S4673	S4768
Junction Depth (μm)	4	10	23
Stripe Width (μm)	85	50	50
Contact Resistance (mohm)	14	12	9
Lowest Frequency (cm^{-1}) at 15K	350	341	337
I_{th} (mA) at 15K	137	117	86
Maximum Power Out (μW) at 15K	320	350	190
Power/Mode at 28 μm (μW) *	68	47	80
Maximum CW Temperature (K)	73	74	60
Highest Frequency (cm^{-1})	544	550	521

* Mode shown cross-hatched on spectral curves

TABLE 6

Summary of physical, electrical and optical characteristics of three regular cavity (RC) mesa stripe lasers fabricated during the early part of the program.

area at a distance of approximately 4 cm from the laser (14° FOV). For laser 3349-28 the beam appeared to point upwards 15° with a vertical (in the junction plane) angle of 60° , while in the horizontal plane (perpendicular to the junction) the beam was centered at 0° with a spread of approximately 70° . Laser 3350-02 had a similar beam spread, with a direction approximately 5° up in the vertical, while laser 3350-17 had a beam center pointing about 10° to the right (as viewed from the window of the laser) with a similar spread.

The emission spectra observed from these lasers are shown in Figures 2 through 6. Laser 3349-28 emitted in single mode at 150 mA, 15K, with an output power of 25 μ W. The power per mode increased to 68 μ W at 1 amp although at that current a number of modes exist. The spectra of this laser are shown in Figures 2 and 3. At the maximum CW operating temperature of 73K this laser emitted at 544 cm^{-1} .

The evolution of a typical emission spectrum with increasing laser current was measured for laser 3350-02, and is shown in Figure 4. The laser operates almost single mode at 150 mA, with 25 μ W of output power. The 343.7 cm^{-1} mode which exists at 150 mA shifts to 344.1 cm^{-1} at 1A, thus giving a mode tuning range of 0.4 cm^{-1} with a current tuning rate of 14 MHz/mA, quite low for diode lasers but not entirely unexpected since the junction depth was quite shallow (4 μ m, see Table 6). The shallower the junction the less the mode tuning rate. Slower tuning rates ease the stability requirements on the laser power supply and provide improved operating stability. Electron-hole recombination in narrow-gap semiconductors is thought to be due to non-radiative Auger recombination which generates heat in the vicinity of the junction. This heat must pass through approximately 4 μ m of $\text{Pb}_{0.9}\text{Sn}_{0.1}\text{Se}$ material before being removed by the OFHC copper heat sink.

Since the thermal conductivity of most solids peaks around 20K, the thermal properties are favorable for efficient heat removal. The current

OF POOR QUALITY

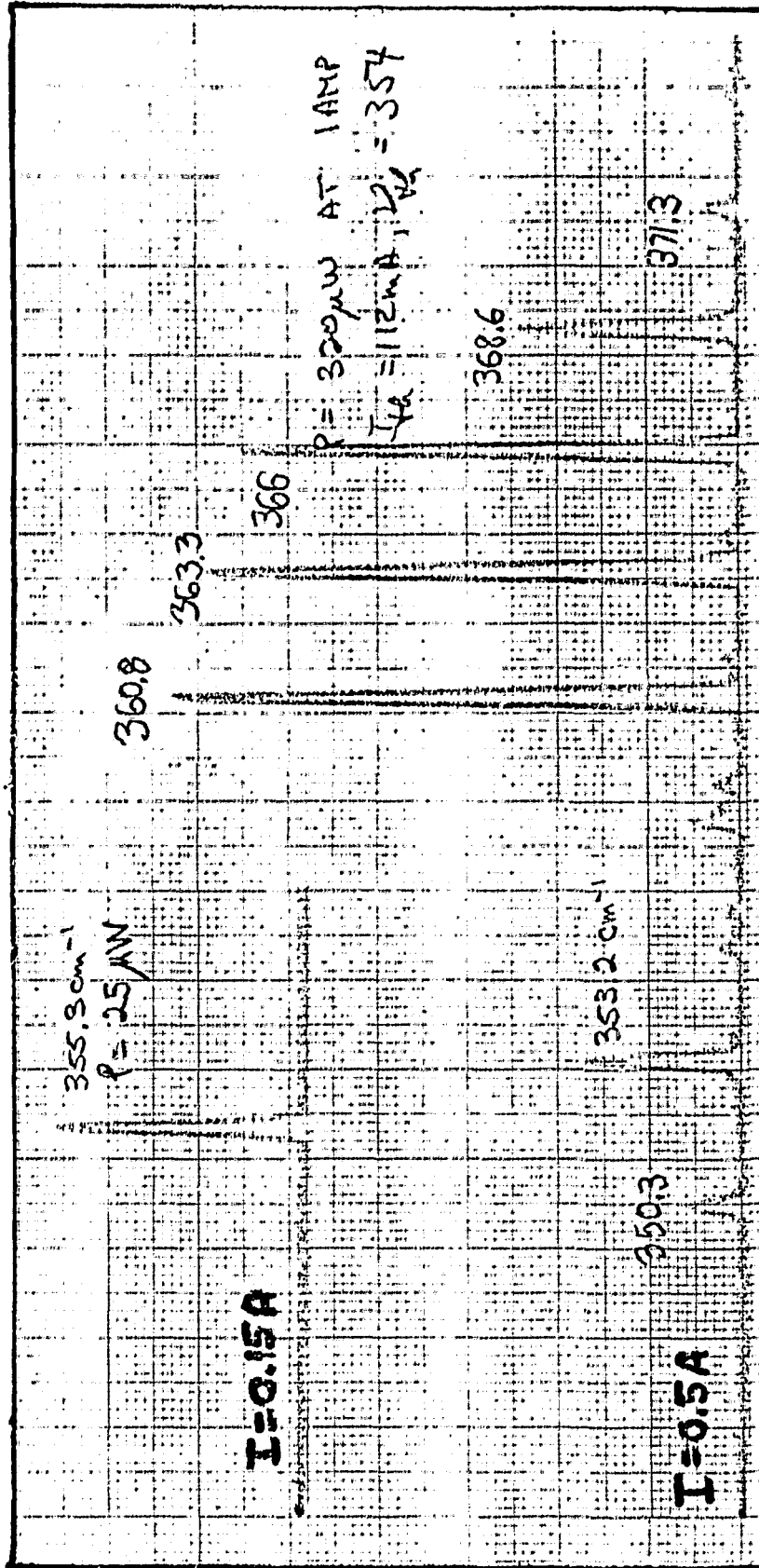


Figure 2

Emission spectra of laser 3349-28
 at 15K and at 2 different values
 of laser current: 0.15A and
 0.5A

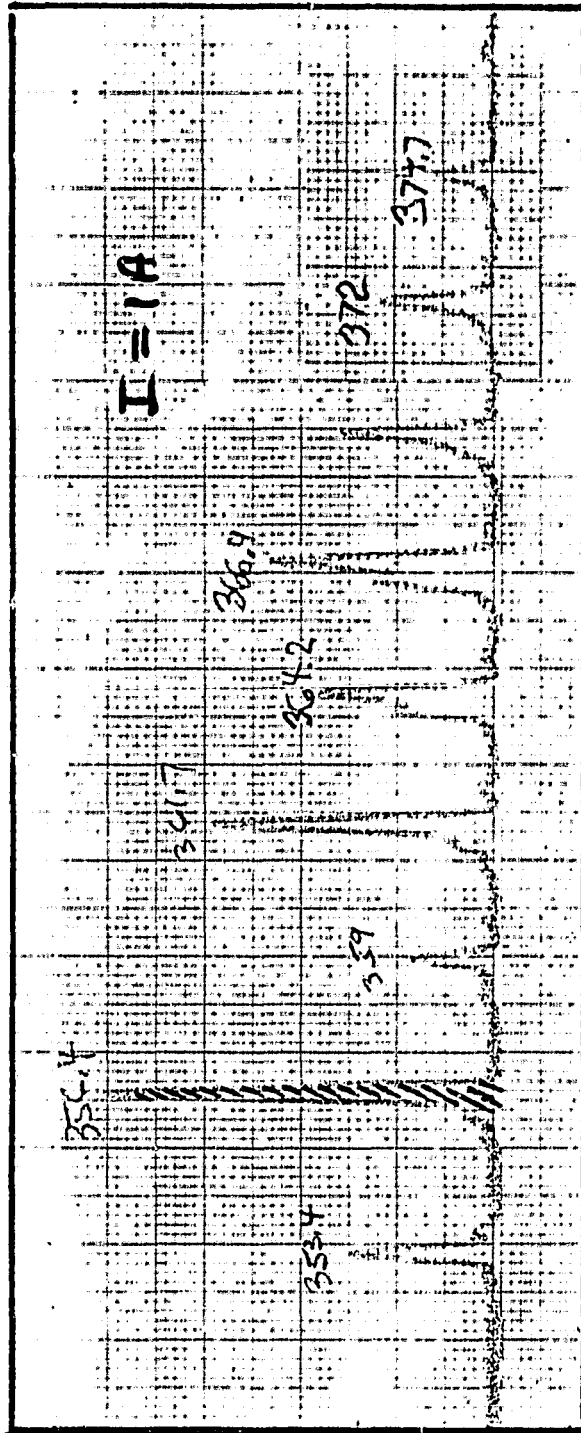


Figure 3

emission spectrum of laser
3349-28 at 15K and 1A. Total
power at 1A is 320 μW

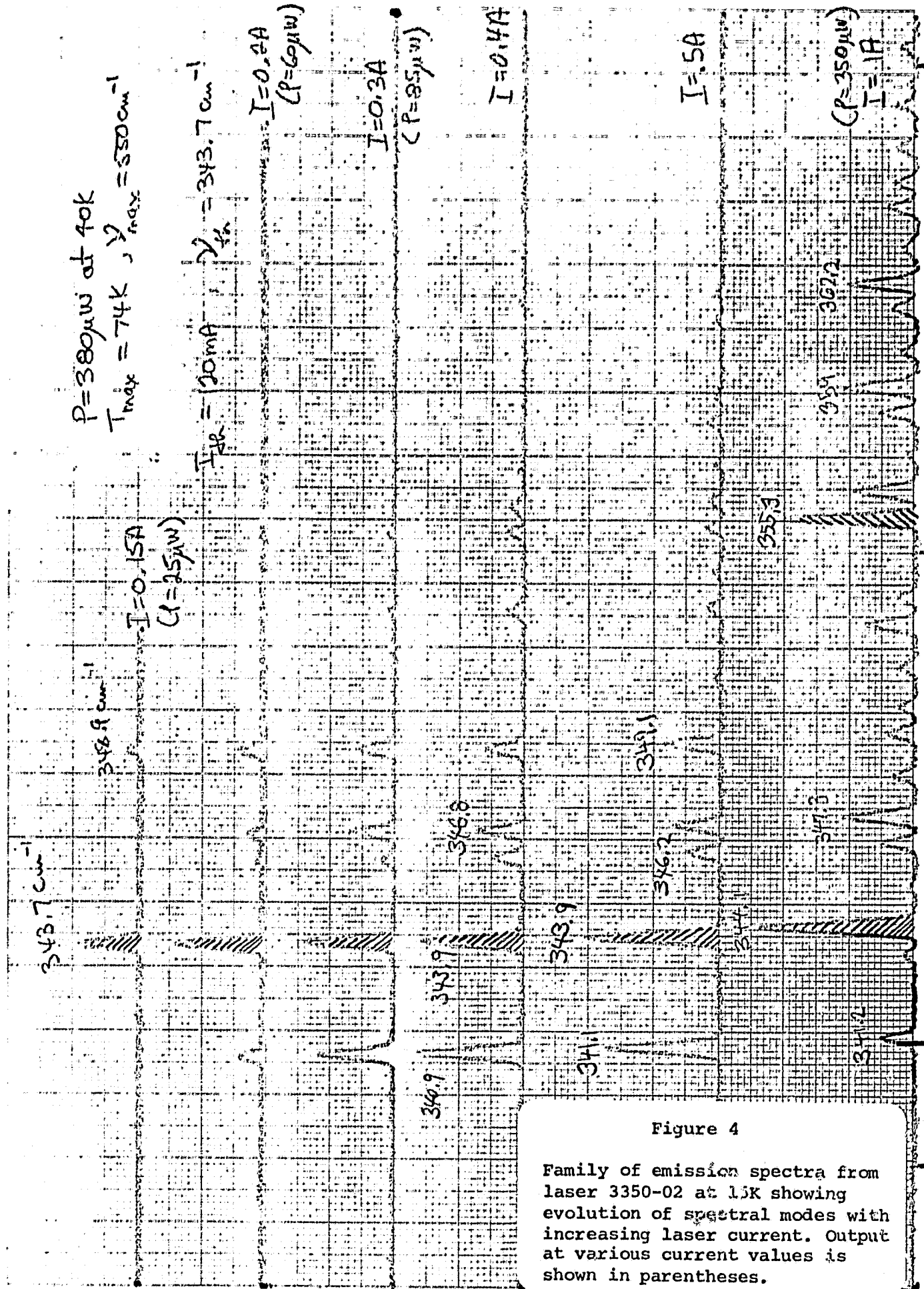
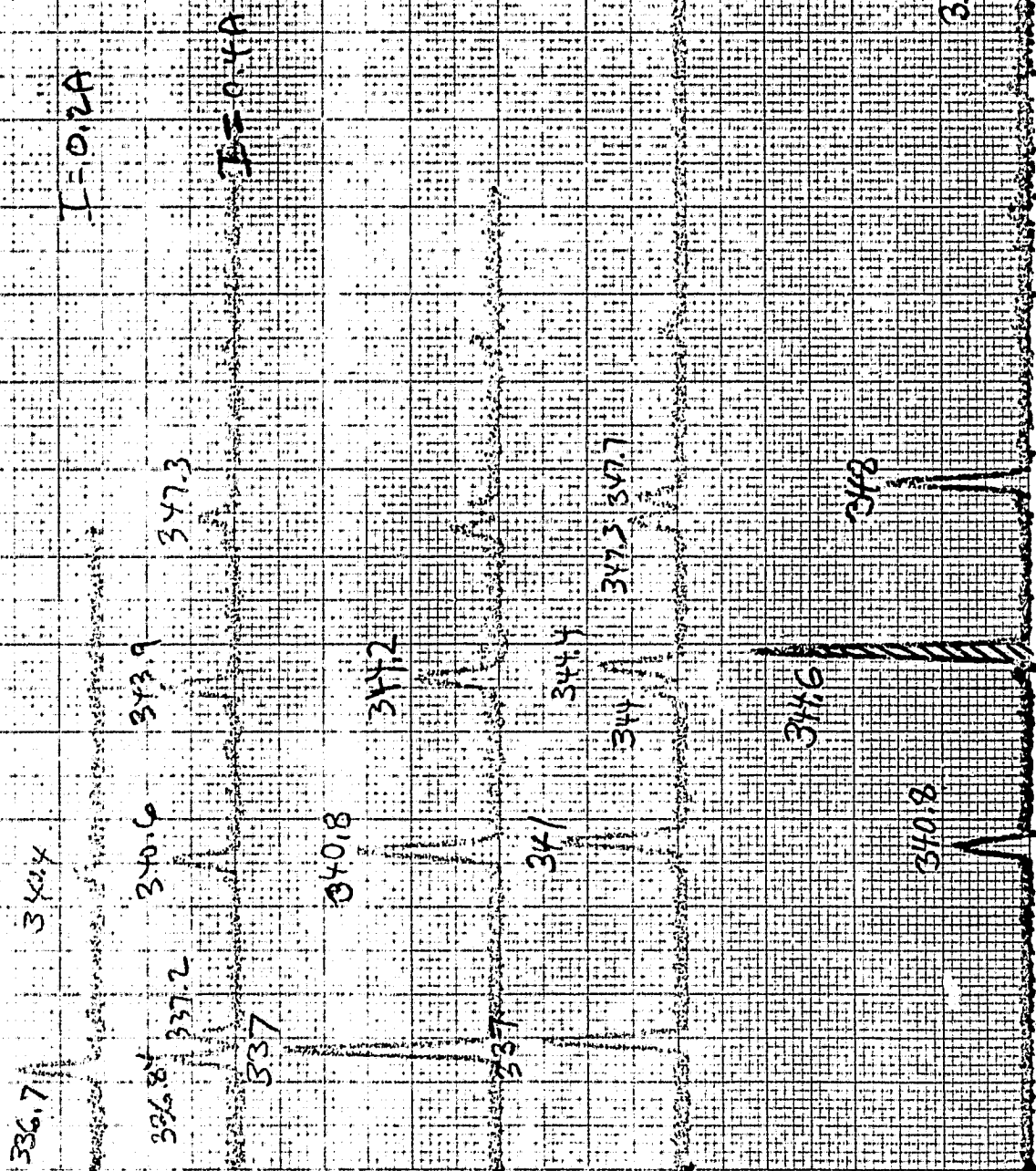


Figure 4

Family of emission spectra from laser 3350-02 at 15K showing evolution of spectral modes with increasing laser current. Output at various current values is shown in parentheses.

Figure 5
Emission spectra of laser
3350-17 at 15K

$I_{th} = 111 \text{ mA}$, $\nu_{th} = 336.7 \text{ cm}^{-1}$



ORIGINAL PAGE IS
OF POOR QUALITY

46 1323

10 X 10 TO 1/2 INCH 7 X 1/2 INCH
K-EF KEUFFEL & ESSER CO. MADE IN U.S.A.



Figure 6

Emission spectra of laser 3350-17
at 25K. Longitudinal mode
separation is 3.5 cm^{-1} .

tuning rate of a single laser mode is given by

$$\frac{dv}{dI} = \frac{dv}{dT} \frac{dT}{dI}$$

Since the laser voltage is essentially constant,

$$\frac{dT}{dI} = V\theta_{th}$$

where θ_{th} is the thermal resistance (K/W) and V is the laser voltage. $\frac{dv}{dT}$, the temperature tuning rate is approximately $0.6 \text{ cm}^{-1}\text{K}^{-1}$. For this laser we measured a current tuning rate of 14 MHz/ma, which implies a thermal resistance θ_{th} , of approximately 16 K/W (K in Kelvins, W in watts). At a full current of 1A, the heat generated at the junction is 50 mW. An additional 14 mW of heat is generated at the contacts. With a $\theta_{th} = 16 \text{ K/W}$, the temperature of the junction is only approximately 1 K above that of the heat sink.

An additional observation of interest regarding laser 3350-02 is that the output power increased with current from 350 μW at 15K to 380 μW at 40K, above which the power began to gradually decrease until, above 74K, CW operation ceased (at 1A).

Figures 5 and 6 show the emission spectra of laser 3350-17, the last of the 3 regular cavity lasers. This laser exhibited the lowest starting frequency, 337 cm^{-1} corresponding to a wavelength of $29.7 \mu\text{m}$. Of the 3 regular cavity lasers, this device has the highest power per mode (80 μW) at $28 \mu\text{m}$, as can be seen from Figure 5 at 1A. Near threshold, where the laser ran in single mode, the output was only 10 μW , however. In this Figure as well as in Figure 6, it can be seen that the mode separation is even, and has a value of approximately 3.5 cm^{-1} , corresponding to an effective refractive index of 6.7 for a $210 \mu\text{m}$ long laser cavity.


4.2 Narrow-Stripe Lasers

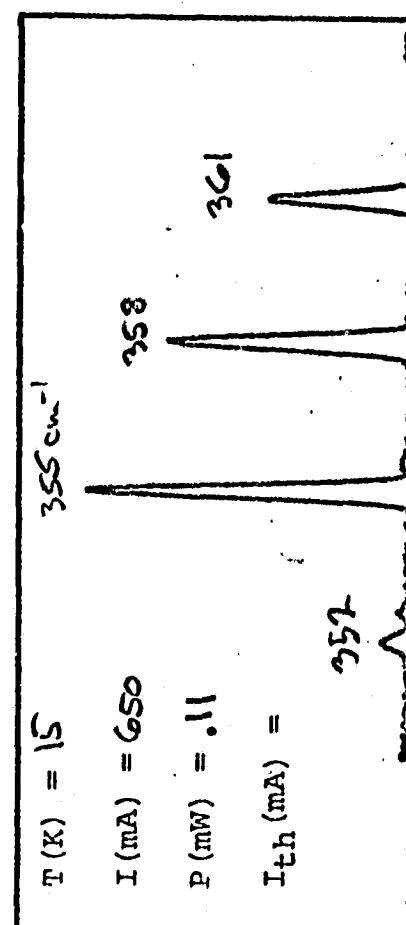
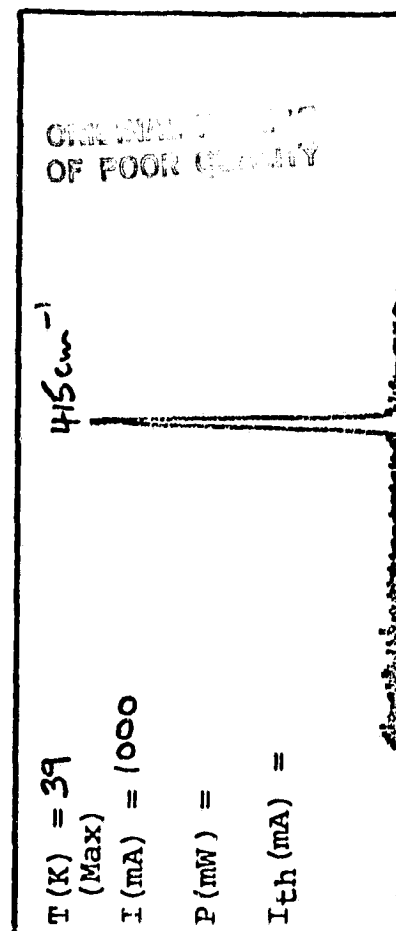
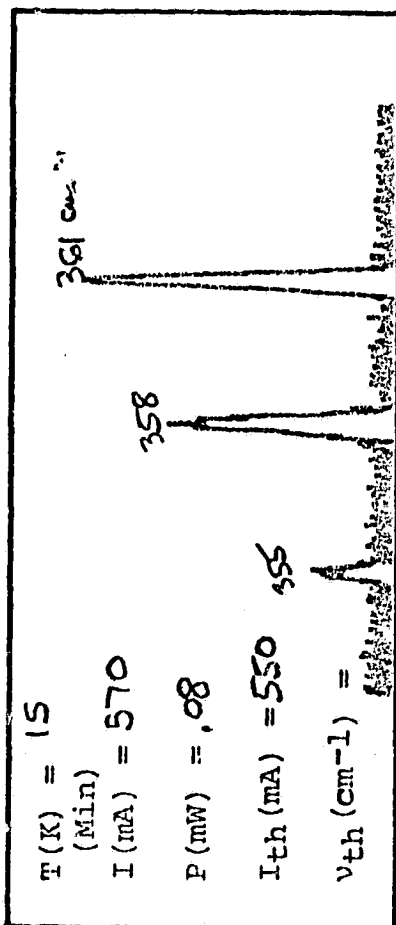
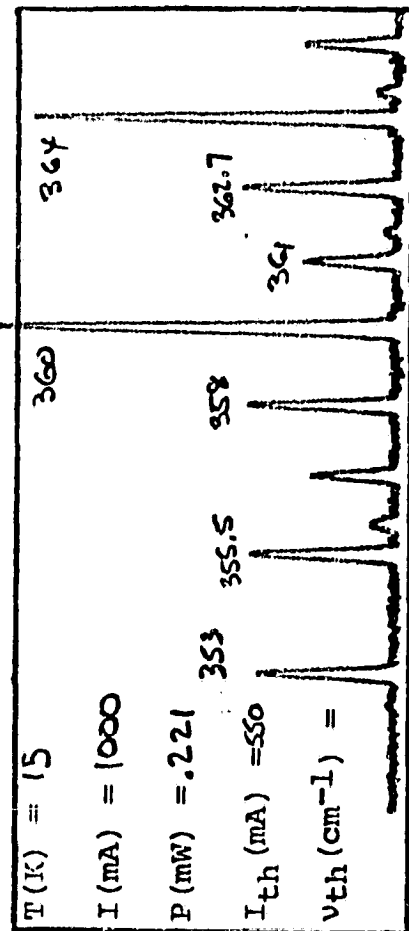
As shown in Table 5, two narrow-stripe (NS) lasers with regular cavity length (250 μm) were fabricated and investigated. These lasers, 4079-13 and 4090-19, exhibited evenly spaced longitudinal mode separation, similar to that observed in the wider-striped lasers discussed in the previous section. The detailed emission spectra of these lasers are shown in Figures 7 and 8. The far field pattern of both of these lasers were centered near 0° with beam spreads of approximately 60° . It will be shown in the next section that short cavity lasers from these same wafers yielded improved performance in terms of single mode operation and output power.

In order to monitor the evaluation of the emission spectrum shape with increasing current, a series of spectra as a function of laser current were taken for laser 4079-13. This family of spectra is shown in Figure 9. The current tuning rate for this laser can be seen to be 20 MHz/ma, similar to that for laser 3350-02 and quite low compared to that usually measured in shorter wavelength lasers. We will see in the next section, that shorter cavity lasers exhibit higher tuning rates due to the expected increase in thermal spreading resistance.

4.3 Short-Cavity Lasers with Narrow Stripes


Bars of the striped wafers used to fabricate the lasers discussed in the previous section (whose assembly was described in section 3.2) were cleaved into cavity lengths of approximately 120 μm . These lasers represent the shortest cavity, narrowest stripe long wavelength lasers assembled to date. Two lasers were fabricated: laser 4094-01 from wafer 4944 and laser 4094-07 from wafer 4946. The far field emission patterns of these lasers were quite similar to those of the previously described longer cavity narrow stripe devices. The emission spectra of these short cavity lasers were quite different than those of longer cavities. The separation between longitudinal modes at high current levels was approximately 6 cm^{-1} , in

 <p>Laser Analytics 25 Wiggins Avenue Bedford, MA 01730 (617) 275-2650 / Telex: 923324</p>	
<p>OPTICAL TEST CONDITIONS</p>	
GRATING	<u>22.5</u>
ORDER	<u>1</u>
FACTOR	<u>HP 85 cal,</u>
WINDOW	<u>KRS-5</u>
TEMP. SENSOR	<u>Si</u>
TEST DATE	<u>3-29-84</u>
TESTED BY	<u>ADP</u>



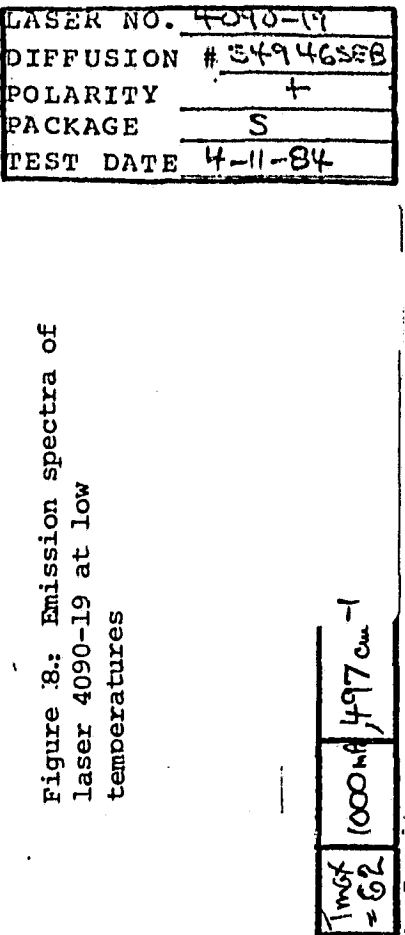
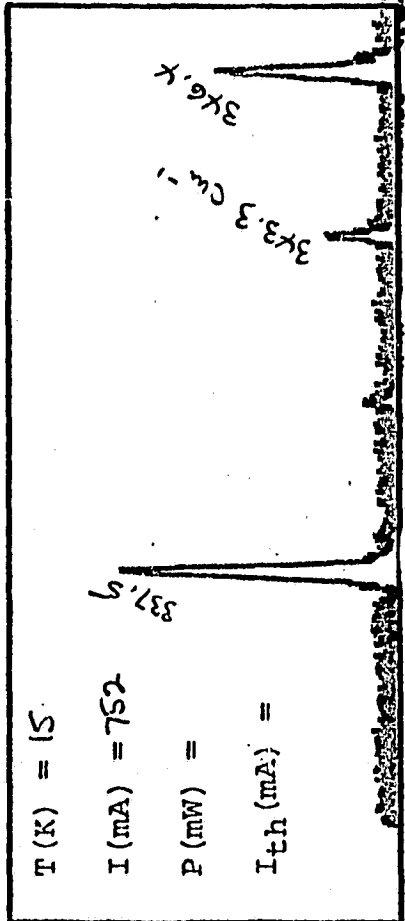
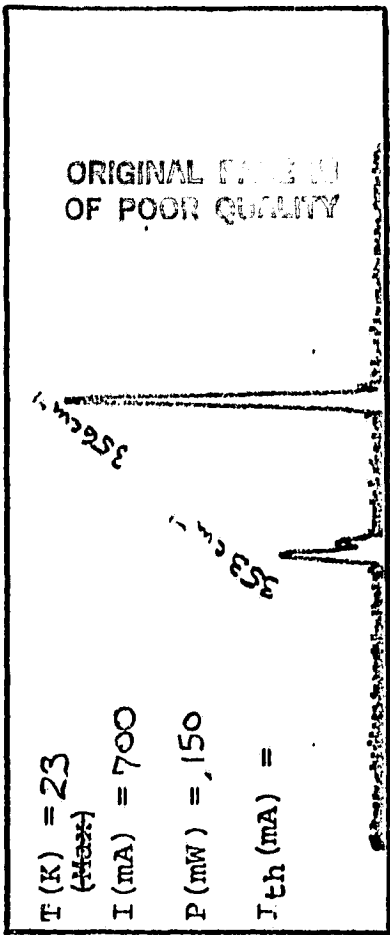
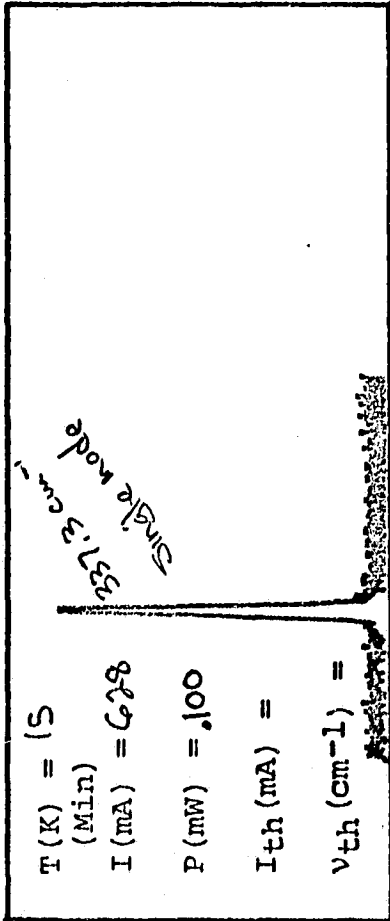
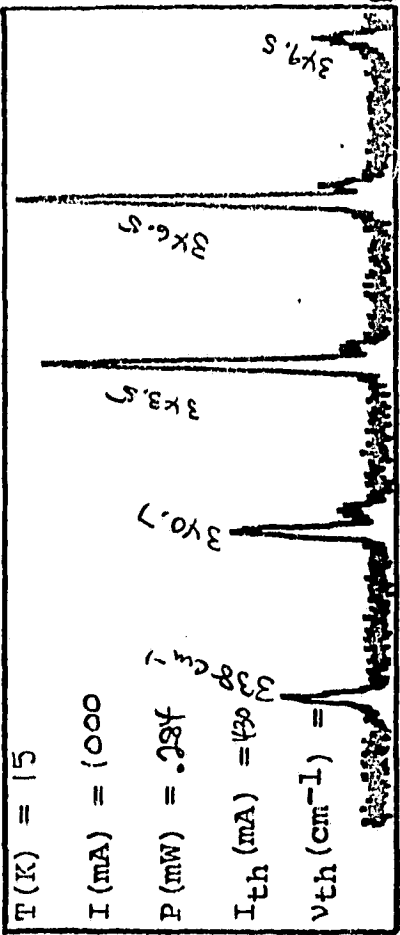
LASER NO.	<u>4079-13</u>
DIFFUSION	<u>#S486XSEB</u>
POLARITY	<u>POS</u>
PACKAGE	<u>S</u>
TEST DATE	<u>3-29-84</u>

Figure 7: Emission spectra of laser 4079-13 at 15K and 39K



Laser Analytics
25 Wiggins Avenue
Bedford, MA 01730
(617) 275-2650 / Telex: 92-3324

OPTICAL TEST CONDITIONS		WINDOW
GRATING	22.5	KRS-5
ORDER	1	TEMP. SENSOR
FACTOR	HP 85 calib.	Si
		TEST DATE
		TESTED BY



CL 100-10
OF 100-10

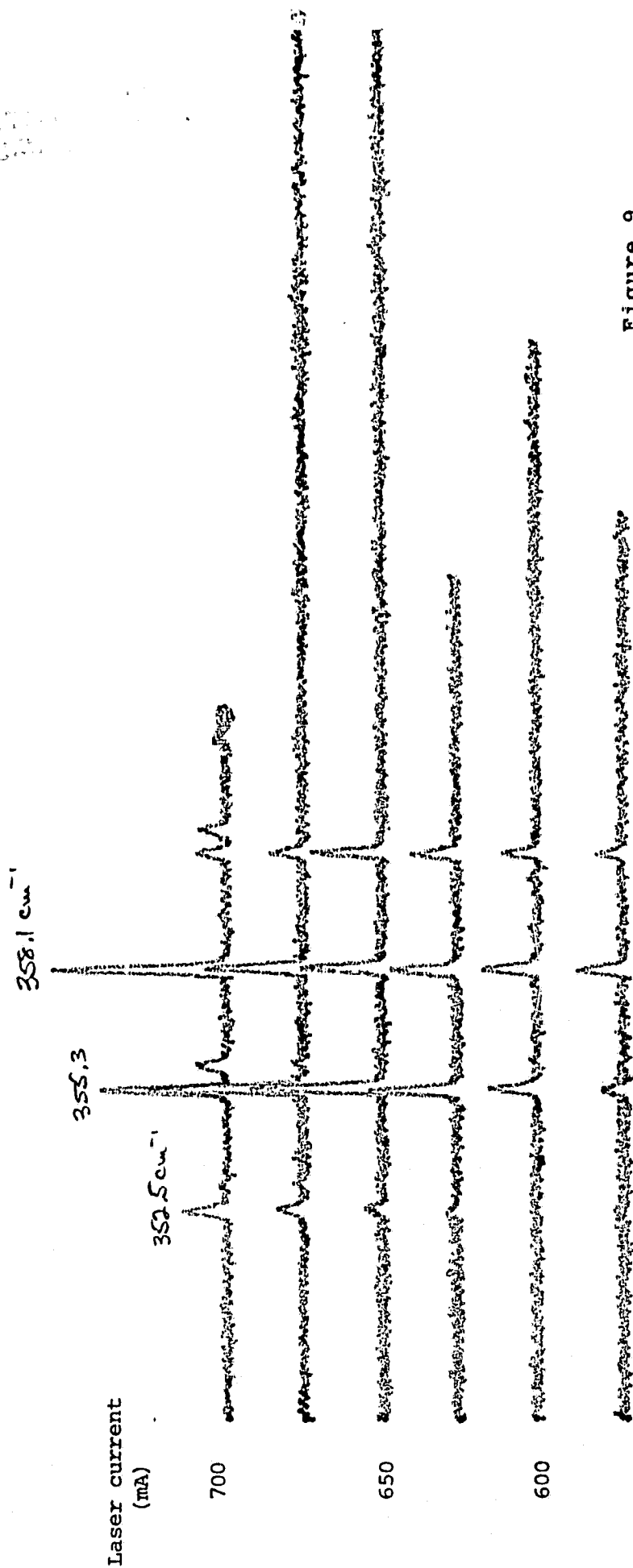
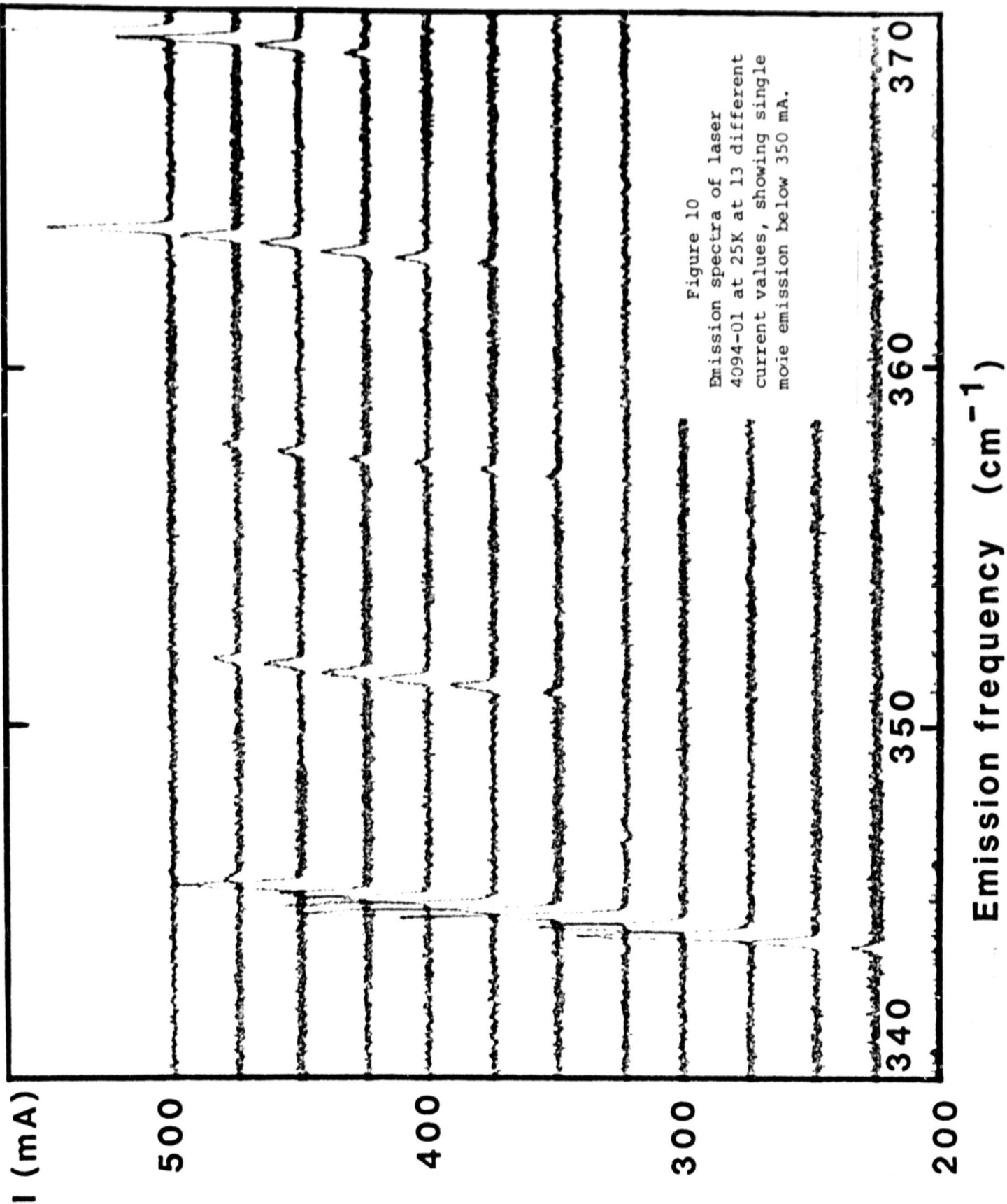


Figure 9

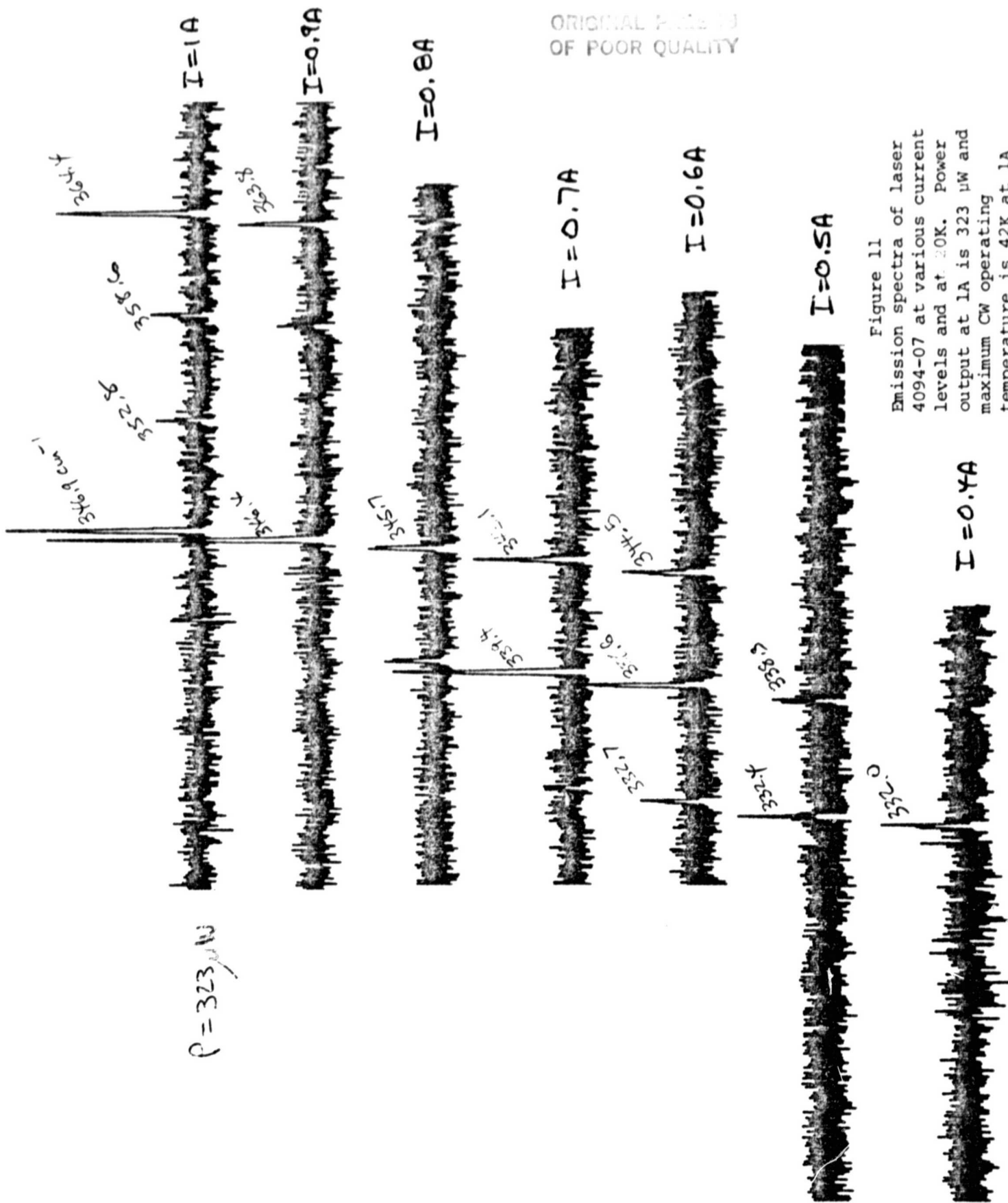
Emission spectra of laser 4079-13 at various current levels, illustrating evolution of the emission spectrum with increasing current. T=15K.

agreement with that expected from a 120 μm cavity length. Such an increase in mode separation reduces the number of modes within the semiconductor gain curve. The evolution of the emission spectrum of laser 4094-01 with current is shown in Figure 10. The most significant feature is that the laser emits in a single mode from a threshold current of 225 mA to a current of approximately 350 mA. Such a broad truly single mode tuning range is usually not encountered in longer cavity lasers. The tuning rate of this mode was 290 MHz/mA. A similar behavior was observed for laser 4094-07. Figure 11 illustrates a longitudinal mode separation of approximately 5.9 cm^{-1} at larger current values, while essentially single mode emission was observed between threshold (250 mA) and approximately 380 mA. Figure 12 shows the detailed spectrum of this laser near threshold. The mode which begins at the 250 mA threshold remains as the dominant mode at up to 500 mA. Tuning at a rate of approximately 130 MHz/mA, somewhat faster than that of the previously noted, larger cavity lasers. Laser 4094-01 was operated at up to 800 mA where the multimode output was 500 μW at 15K.

A comparison of some of the performance characteristics of both narrow striped (NS) and narrow striped short cavity (SC) lasers is shown in Table 7. Both the single mode tuning range and tuning rates are higher for the SC lasers. From the viewpoint of operating in pure single mode over the widest possible current range and at the highest possible power per mode, the SC laser No. 4094-01 had the best performance. The output power of 112 μW in a purely single mode is the highest observed by us to date, and indicates what may be a major advantage of short cavity lasers.



ORIGINAL FILED IN
OF POOR QUALITY



ORIGINAL PAGE IS
OF POOR QUALITY

Figure 11
Emission spectra of laser
4094-07 at various current
levels and at 20K. Power
output at 1A is 323 μW and
maximum CW operating
temperature is 42K at 1A

OF 4094-07

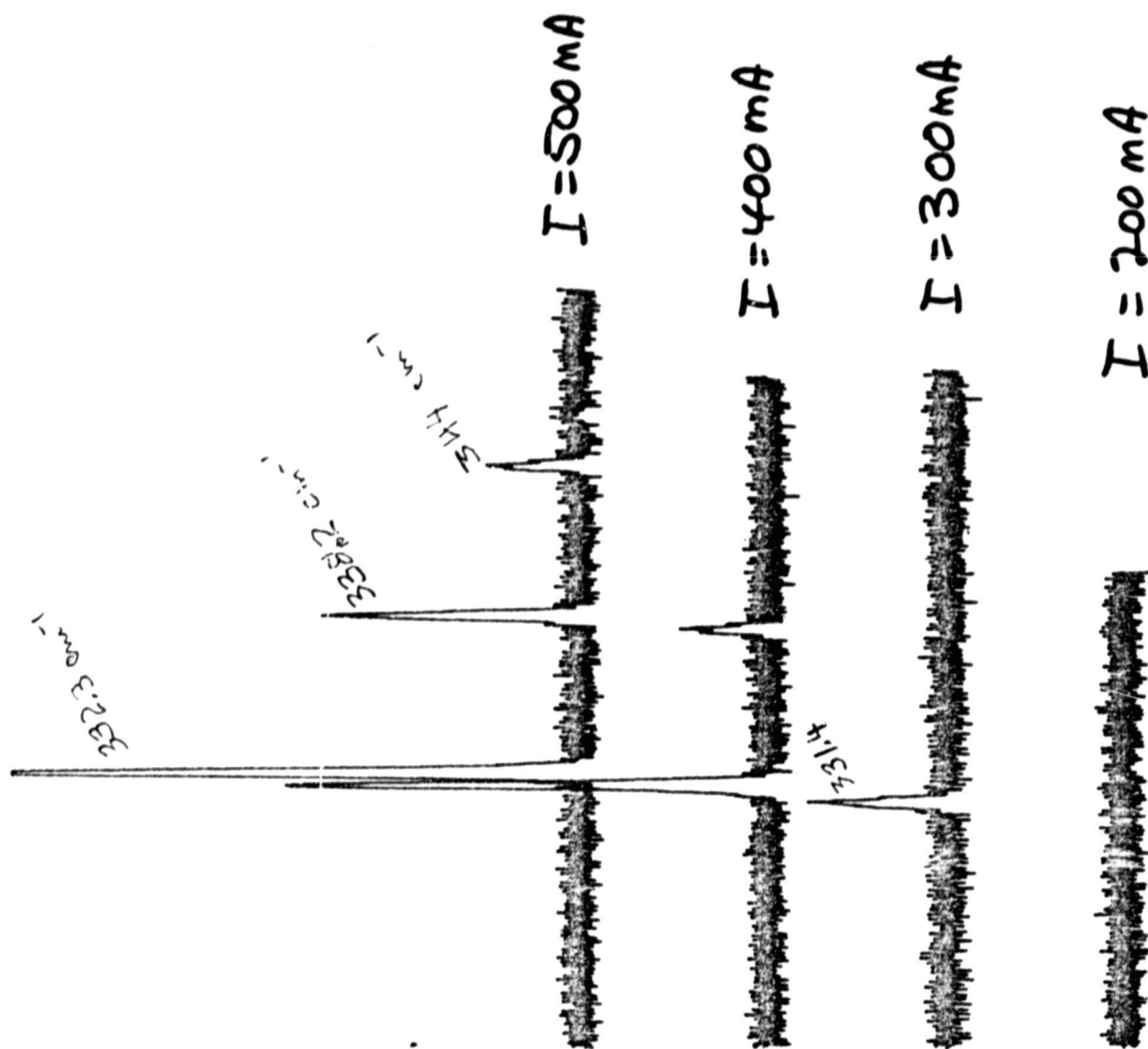


Figure 12
Detailed emission spectrum of
laser 4094-07 at 20K near
threshold. The laser emitted
single mode at approximately
 $30.2 \text{ } \mu\text{m}$ and was tunable over
approximately 1.0 cm^{-1}

Laser No.	Cavity Length (μm)	Single-mode Operating region (mA)	Power in the Single-Mode at highest current in single mode region (μW)	Single Mode Tuning		Separation between modes at higher currents (cm^{-1})
				Range (cm^{-1})	Rate MHz/mA)	
4079-13	250	540-560	26	0.01	20	3.0
4090-19	250	430-628	100	0.17	25	3.0
4094-01	120	225-350	112	1.21	290	6.1
4094-07	120	250-380	56	0.56	130	5.9

TABLE 7

Comparison of performance of narrow mesa-striped (20 μm) lasers with different cavity lengths.

5.0 RETEST OF PREVIOUSLY FABRICATED LASERS

All available lasers fabricated during the past 3½ years of the various contract phases were retested during this past year. Both electrical and optical characteristics were measured for each laser.

In terms of electrical test results, it was found that no increases in contact resistance occurred for any of the lasers. This demonstrates a high level of metallurgical stability of the contact metallization configuration, a fact consistent with our other data on PbSnSe lasers covering a period of over 5 years. Optical test results, summarized in Table 8, indicate that all lasers are operational in the same spectral region as measured immediately after fabrication, and, furthermore, the power levels and maximum operating temperatures of each laser are similar to those originally observed. Three of the lasers listed in Table 8 are at MIT Lincoln Laboratory and therefore did not go through the regular 3 month test intervals, nor were they retested optically. In Table 8, the parameter P_m indicates the maximum multimode laser output power at the lowest temperature (15-20K) while T_m indicates the maximum measured CW operating temperature at 1 amp of laser current. Details of the optical test data summarized in this table are shown in Figures 13-25.

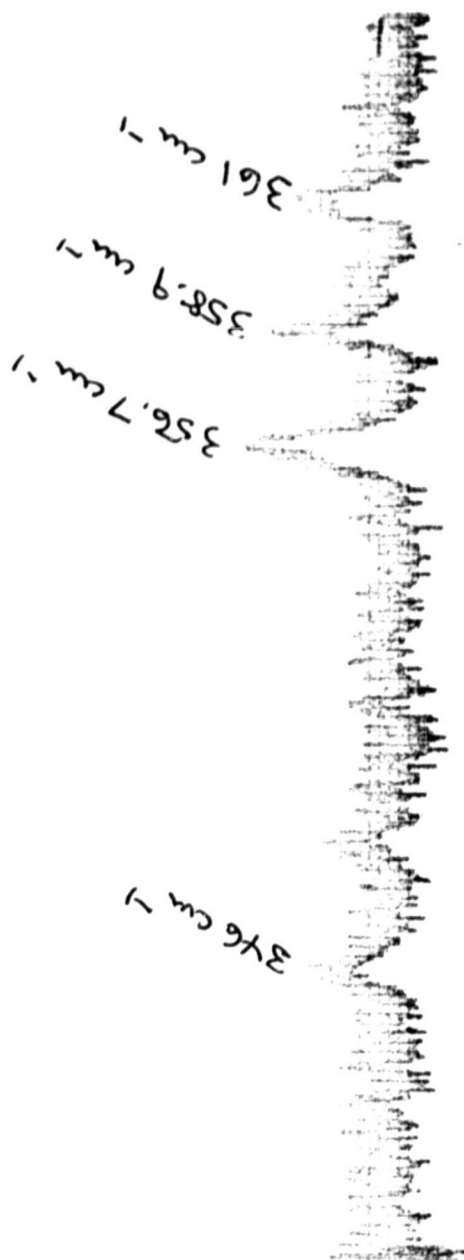
Laser No.	<u>Original Test Data</u>				<u>Retest Data taken during</u> <u>Dec., 1983</u>				
	I_{th} (mA)	Tuning Range ($cm^{-1} - cm^{-1}$)	Pm/Tm ($\mu W/K$)		I_{th} (mA)	Tuning Range ($cm^{-1} - cm^{-1}$)	Pm/Tm ($\mu W/K$)	Age at retest (mo)	
NLW-1	446	344	446	226/47	646	345	445	126/45	38
NLW-3	660	342	447	170/50	891	354	405	80/40	38
NLW-4	at MIT Lincoln Laboratory								
2032-25	354	345	419	120/40	318	346	420	200/40	23
2084-52	492	353	449	270/40	527	350	440	380/40	22
2127-01	at MIT Lincoln Laboratory								
2127-06	401	338	435	257/45	516	340	428	180/40	20
2127-51	514	331	436	240/50	551	326	435	280/50	20
2127-61	at MIT Lincoln Laboratory								
2182-56	487	333	471	200/62	591	332	465	126/62	18
3088-4	960	357	534	250/62	837	351	535	190/62	9

TABLE 8

Optical retest data for lasers fabricated during the past four years on Contract NAS5-26200.

Figure 13: Optical Retest
Data for Laser
NLW-1 at 15K and
1 Amp

$T = 15K, I = 1A$
 $P \approx .06 mW$
 $T_{max} = 45K \text{ (} 445 \text{ cm}^{-1} \text{)}$
 $I_{th} = 650 mA$



$T = 15K$, $I = 2A$
 $P = .126 \text{ mW}$ multimode (lead less/dow)
 $200 \mu\text{m}$ slits

$\nu_{th} = 345 \text{ cm}^{-1}$ @ 1000 mA

Figure 14: Optical Retest
 Data for Laser
 NLW-1 at 15K and
 2 Amps

ORIGIN: 500.0000
 OF POOR QUALITY

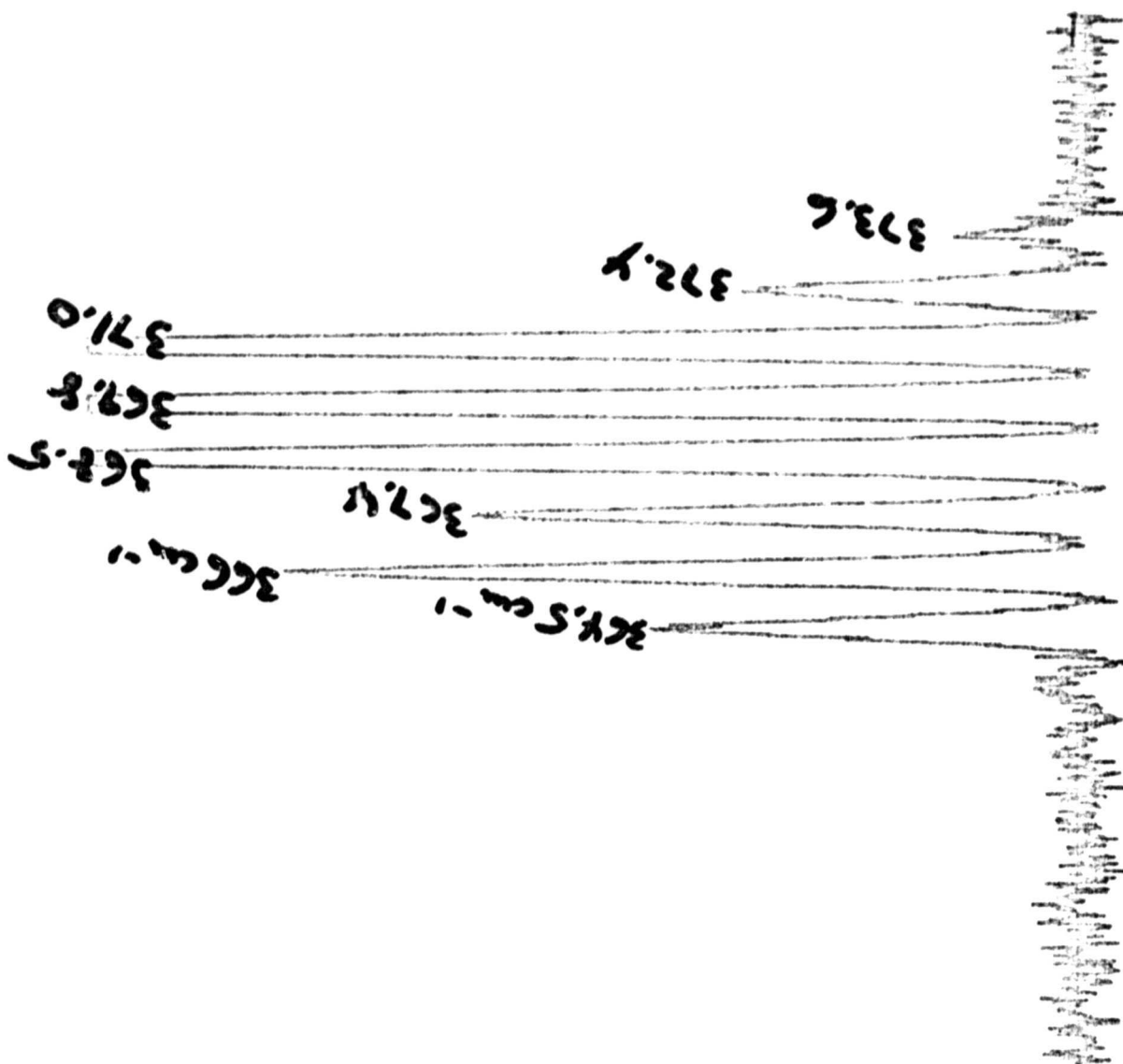


Figure 15: Optical Retest
Data for Laser
NLW-3 at 15K, 2 Amps

$T = 15K, I = 2A$
 $P = .08mW$ multistroke
200 μm slits

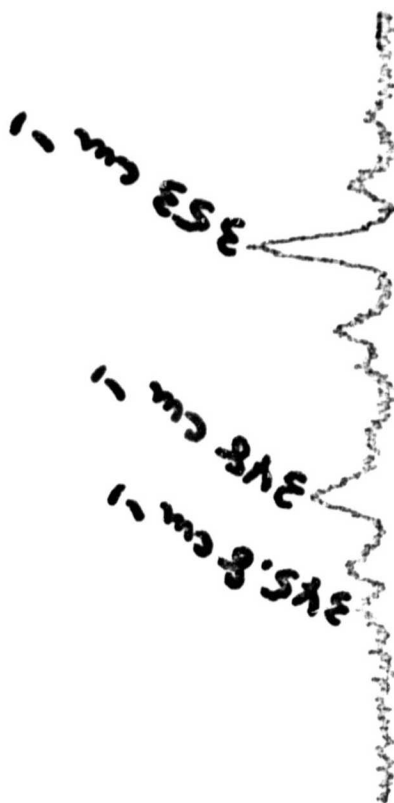
$V_L = 354 cm^{-1}$

$T_m = 40K$
 $\gamma_m = 405$



$T=15K, I=1A$
 $P=.07mW$ multimode
200 μm slits

Figure 16: Optical Retest
Data for Laser
2032-25 at 15K,
1 Amp



$T = 15K$, $I = 2A$
 $P = 20mW$ multimode
200 μm slits

$T_m = 40K$
 $V_{max} = 420$

Figure 17: Optical Retest
Data for Laser
2032-25 at 15K,
2 Amps



Figure 18: Optical Retest
Data for Laser
2084-52 at 15K,
2 Amps

$T \approx 15K$, $I \approx 2A$
 $P = .380mW$ multimode
 200 μm slit
 $T_{max} = 40K$
 $V_{max} = 440$

OF FOUR QUALITY

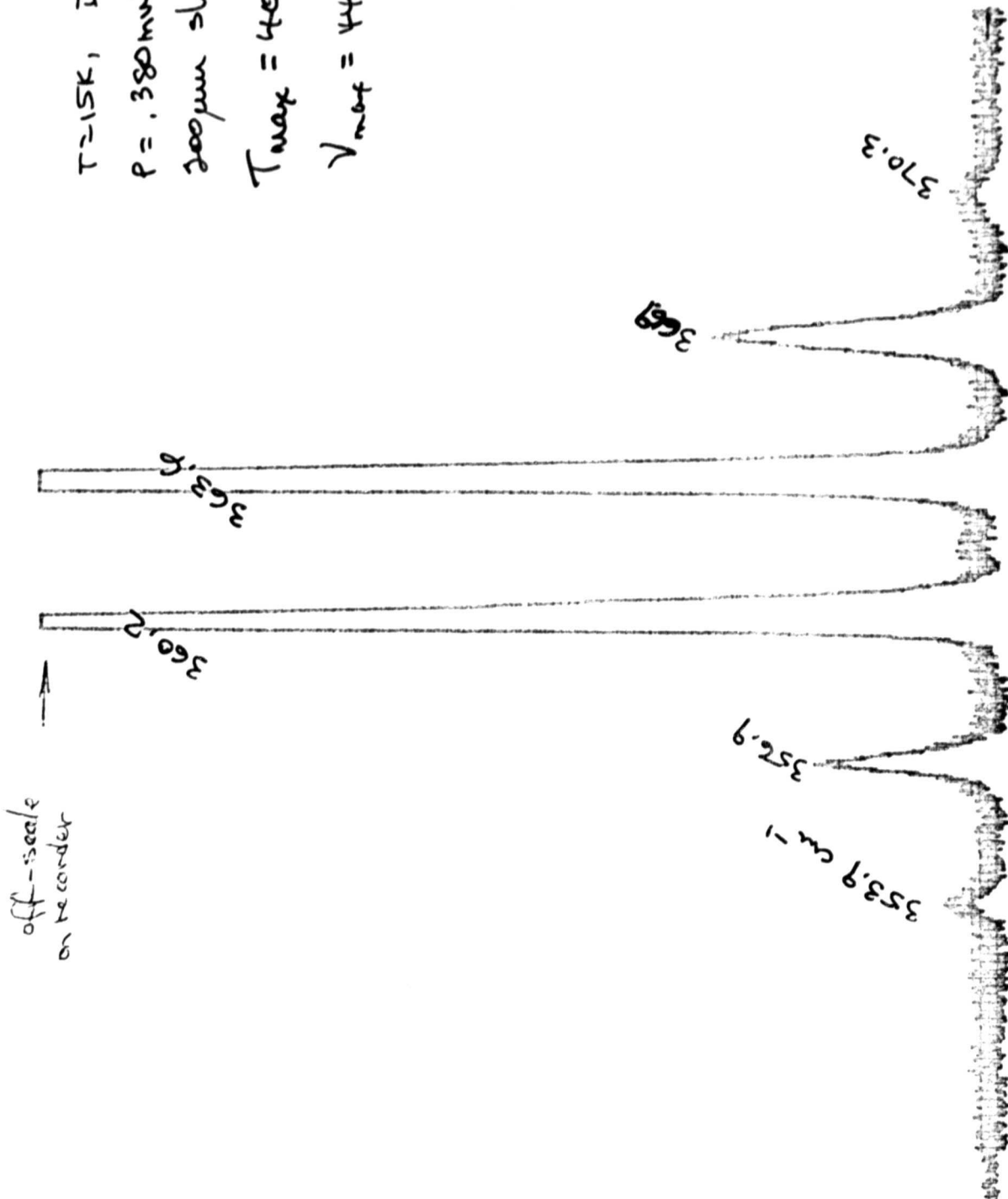


Figure 19: Optical Retest
Data for Laser
2084-52 at 15K,
0.90 Amps

$T = 15K$, $I = 0.90A$
200 μm slit widths

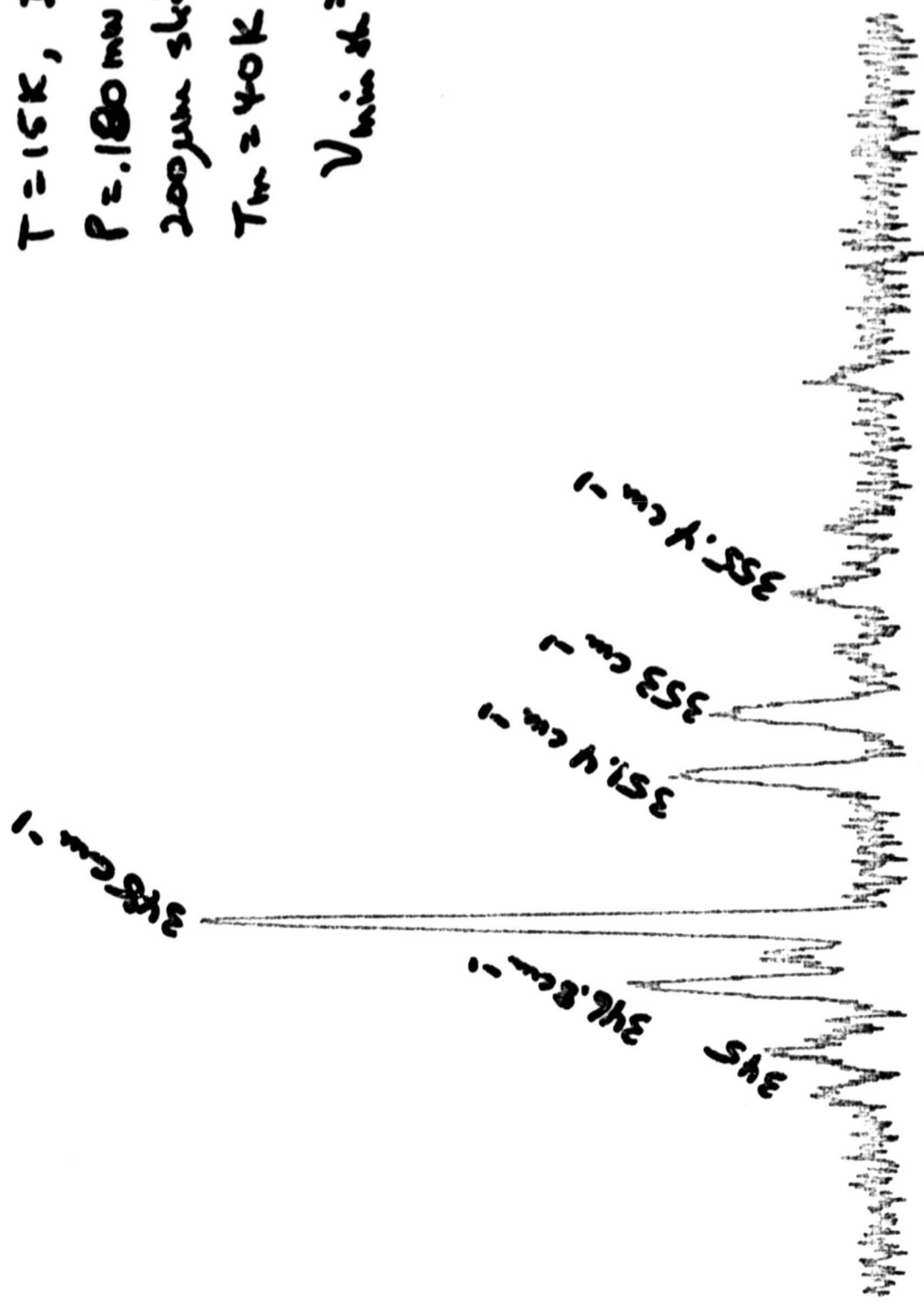
ORIGINAL DATA
OF POOR QUALITY



$T = 15K$, $I = 1.9A$
 $P = 180mW$ multimode
 $200\mu m$ slits
 $T_m = 40K$, $V_{max} = 428$
 $V_{min} = 340$

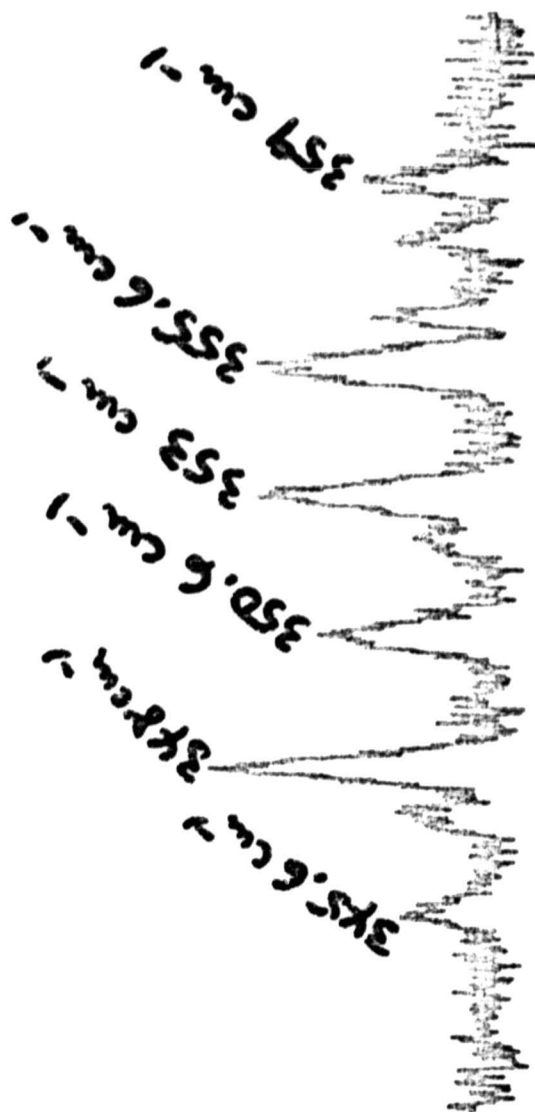
ORIGINAL
 OF POOR QUALITY

Figure 20: Optical Retest
 Data for Laser
 2127-06 at 15K,
 1.9 Amps



$T = 27K$, $I = 1.9A$
 $P = 0.25mW$ multimode
 $200\mu m$ slits
 $(T_m = 50K)$
 $\lambda_m = 435$

Figure 21: Optical Raman
 Data for Laser
 2127-51 at 27K,
 1.9 Amps



$T = 15K$ $I = 1.88$ Amps
 $P = 0.28$ mW multivode
200 μ m slits
($T_n = 50K$)

Figure 22: Optical Retest
Data for Laser
2127-51 at 15K,
1.88 Amps

ORIGINAL P
OF POOR Q

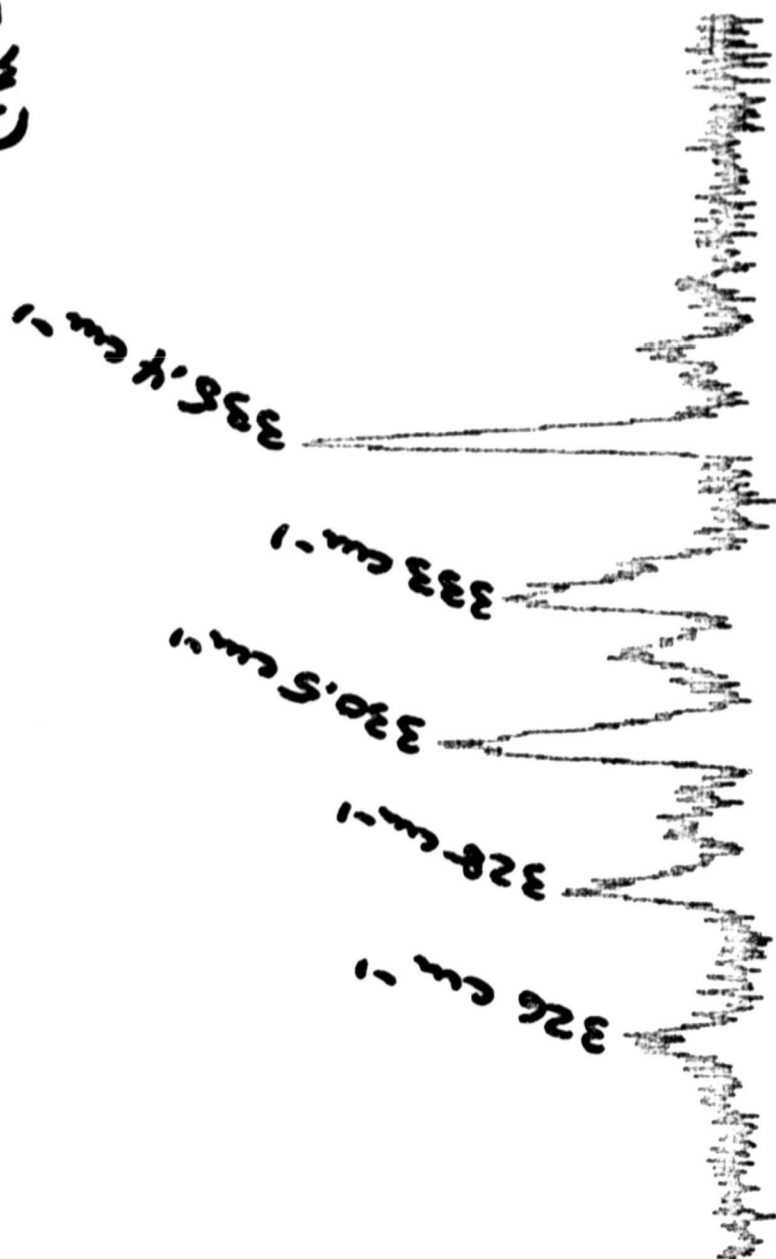


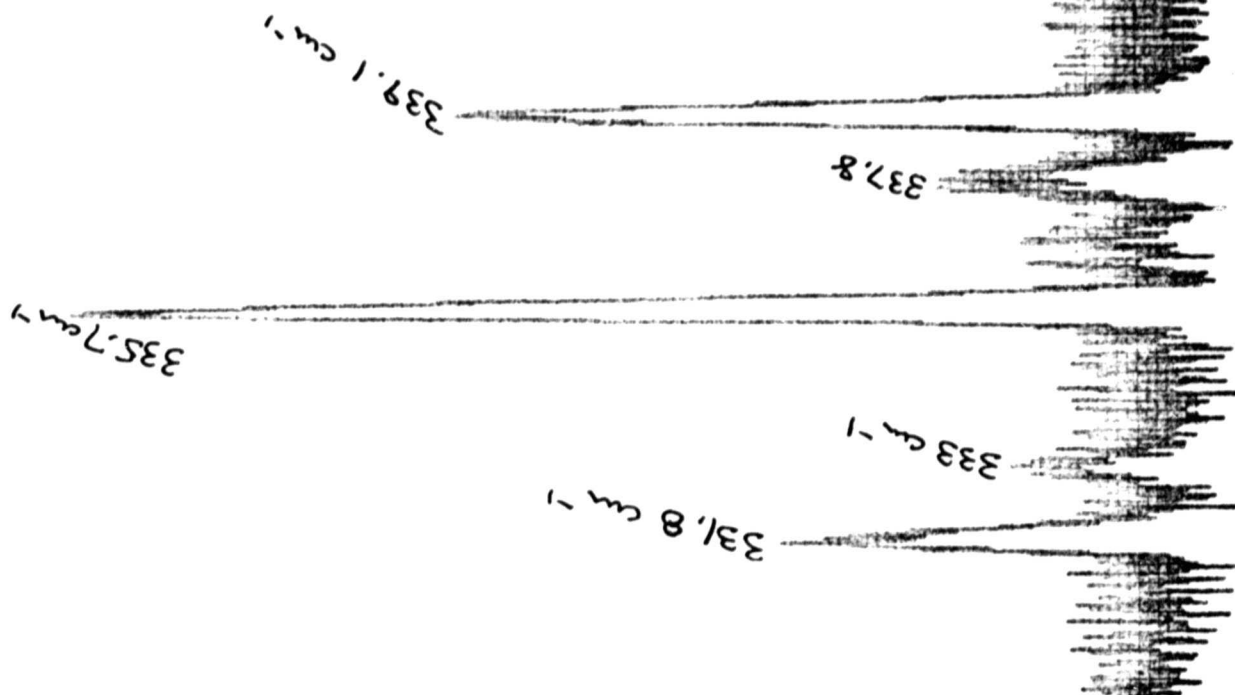
Figure 23: Optical Retest
Data for Laser
2182-56 at 15K,
2.0 Amps

$T = 15K$, $I = 2A$
 $P = .126mW$ multimode
slits = 200 μm

$I_{th} = 500mA$
 $V_{th} = 333cm^{-1}$

$T_{max} = 62K$
 $V_{max} = 465cm^{-1}$

ORIGINAL DATA
OF POOR QUALITY



$T = 15K$, $I = 2A$
 $P = 0.190 \text{ mW, multi mode}$
 $T_{max} = 62K$

OF 100% (0.001)

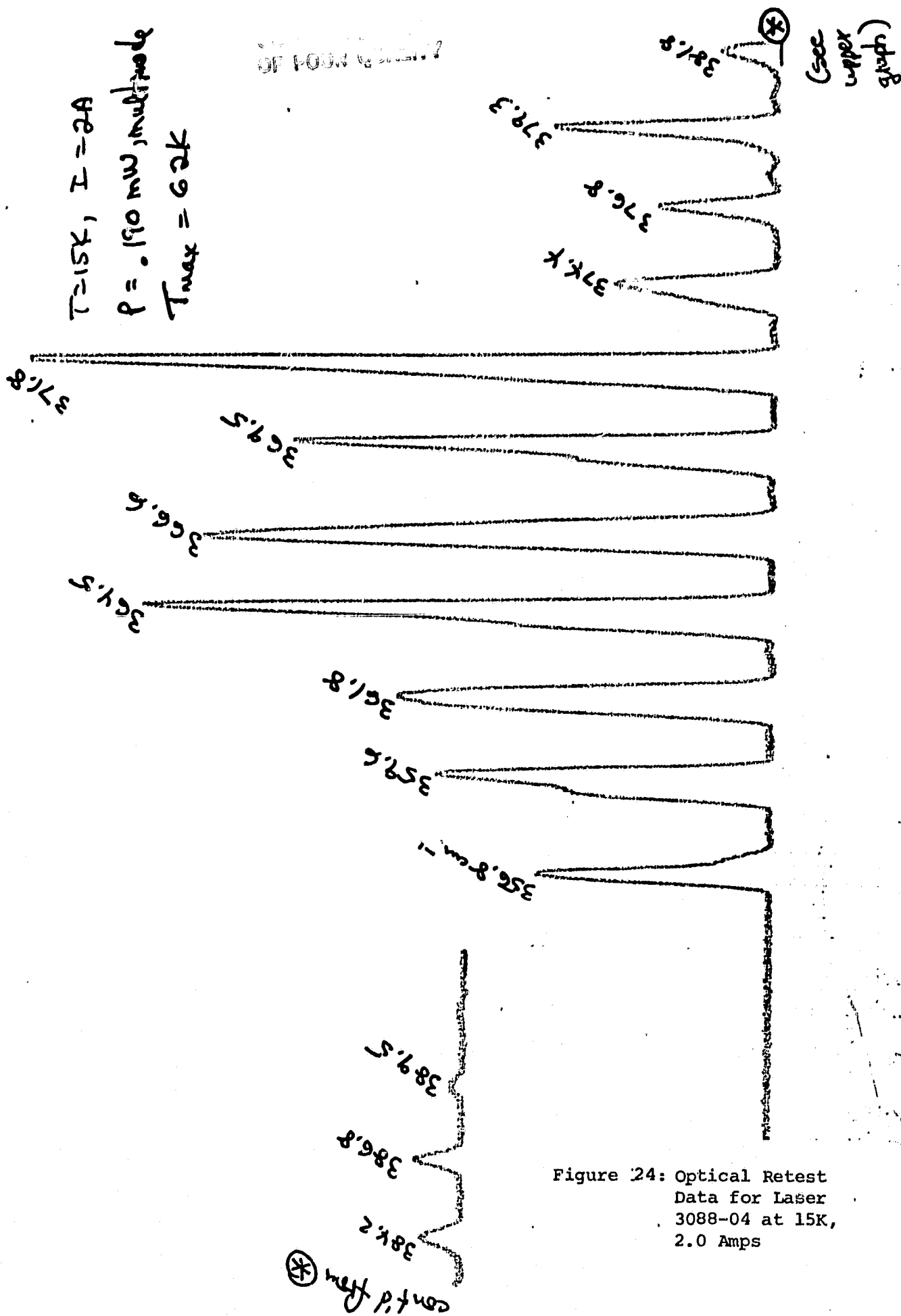


Figure 24: Optical Retest
 Data for Laser
 3088-04 at 15K,
 2.0 Amps

$T = 15K$, $I = 1.0A$
 $P = .08mW$ multimode
 $T_{max} = 62K$

ORIGINAL FIGURE
OF POOR QUALITY

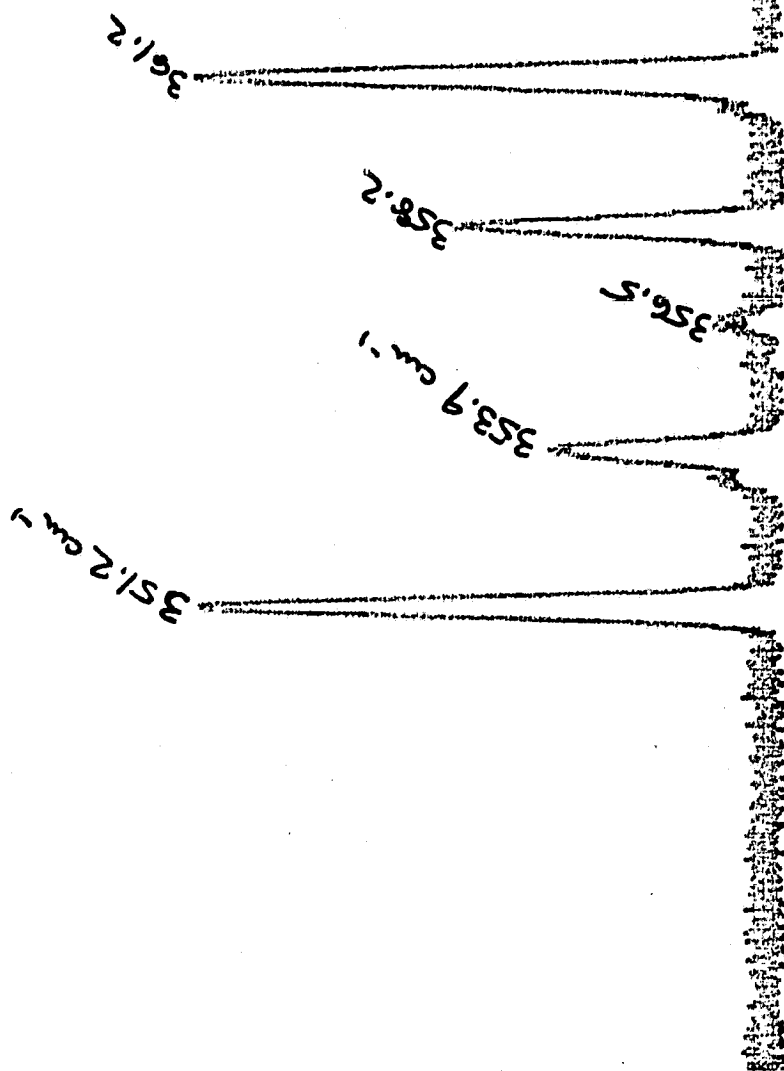


Figure 25: Optical Retest
 Data for Laser
 3088-04 at 15K,
 1.0 Amps

6.0 DELIVERABLE LASERS

A list of the lasers fabricated during this contract amendment period is given in Table 9. Laser 4079-13, fabricated from wafer S4864SEB exhibited evidence of degradation on electrical retest. Examination of the processing records for this wafer indicated that some peeling of the metallization layers occurred during the laser fabrication operation. These data are consistent with data from other wafers included in the same metallization run, which also yielded lasers which degraded.

The other six lasers of Table 9 were, upon request by David Spears of the MIT Lincoln Laboratory and in accordance with the contract instructions, delivered to Lincoln Laboratory for use in the Spears' heterodyne detection apparatus.

Laser No.	Cavity (μm)		T_{max} (K)	CW Spectral Coverage (cm^{-1})	P_{max} (μW) Multimode	P_{max} (μW) single mode
	length	Width	CW			
3349-28	210	85	73	350-544	320	25
3350-02	210	50	74	341-550	350	25
3350-17	210	50	60	337-521	190	10
4079-13	250	20	39	353-415	221	26
4090-19	250	20	23	337-356	284	100
4094-01	120	20	NA	343-NA	500	112
4094-07	120	20	42	331-NA	323	56

TABLE 9

List of lasers fabricated during the contract period and some of their performance parameters. All of these lasers, with the exception of unit 4079-13 were delivered to MIT Lincoln Laboratory.

7.0 SUMMARY AND CONCLUSIONS

We have successfully extended the narrow mesa stripe technology to lasers operating in the 28 μm spectral region. Such lasers exhibited particularly favorable operating parameters when their cavity lengths were reduced to 120 μm . Devices with true single mode emission over current ranges of 120 mA above threshold were obtained, yielding single mode output power levels as high as 112 μW . It was found that the single mode tuning rates of short cavity devices were from 5 to 10 times higher than for long cavity lasers. A comparison of the general contract goals and actual achievements is shown in Table 10.

Excellent long-term operating stability was demonstrated by retesting all in-house lasers fabricated during the various program phases, extending back almost 4 years. In every case the laser emission characteristics were such that the same spectral ranges and power levels as originally observed immediately after fabrication were demonstrated on lasers as old as 3 years.

TABLE 10

Comparison of contract goals and actual achievements during the contract period.

Contract Goal	Achieved
(a) Determine optimum stripe width	Stripe widths of 20 μm yielded the best results in terms of single mode operation and single mode power.
(b) Determine optimum laser cavity length	The shortest cavity (120 μm) yielded lasers with the best single mode characteristics including a single mode output power of 112 μW in the 28-29 μm spectral region
(c) Utilize junction diffusion sources which avoid previously observed shift towards shorter wavelength	Use of as-grown, p-type crystals, diffused with n-sources consistently yielded lasers with starting frequencies in the 332-350 cm^{-1} region.
(d) Investigate surface treatments to reduce and stabilize leakage currents	The pre-insulator deposition etches resulted in fairly stable leakage currents, as demonstrated by vacuum baking experiments.

8.0 RECOMMENDATIONS FOR FUTURE WORK

We have developed the technology of fabricating long wavelength 28 - 30 μm) diode lasers to the point where single mode emission with output power levels of up to 112 μW have been demonstrated. Such single mode emission was limited, however, to drive current ranges of approximately 120 mA above threshold. Since it will be difficult to achieve either significantly narrower stripes or much shorter cavities (because of chip handling problems), other approaches should be investigated.

With the prime requirements of single mode emission at maximum output power, two approaches appear particularly promising. The first and simplest approach is that of fabricating a laser in the cleaved, coupled cavity (C^3) configuration. We have demonstrated the viability of this method in shorter wavelength (5 μm) Pb-salt materials. This same device structure would be expected to yield single mode long wavelength lasers with limited operating regions. An additional advantage of a device with this structure is that the operator has an additional degree of freedom in mode control.

The second and somewhat more lengthy approach is to develop a true double heterostructure (DH) laser configuration. At the present time the method of liquid phase epitaxy (LPE) appears as the most viable one to achieve such structures. Sufficient phase equilibria information is available to predict that lattice-matched DH structures can be achieved using PbSe substrates. We estimate that a program to develop such a technology for 28 - 29 μm laser fabrication would require approximately 2 years.

REFERENCES

1. T.C. Harman and J.P. McVittie, Jour. Electronic Materials 3, 843 (1974)
2. T.S. Moss, G.J. Burrell and B. Ellis, Semiconductor Optoelectronics, Butterworths, London, p. 84 (1973)
3. K.J. Linden, Jour. Electronic Materials 11, 575 (1982)

APPENDIX

Publications and Talks During the Contract Period

1. K.J. Linden, "Tunable Diode Lasers for 3-30 μm Infrared Operation", presented at 27th Annual Technical Symposium of the International Society for Optical Engineering, August 21-26 (1983), San Diego and published in Proc. SPIE 438, 2 (1983)
2. K.J. Linden, "Semiconductor Lasers - An Introduction", Tutorial T9 given at Technical Symposium East '84, April 30, 1984, Arlington, Virginia
3. K.J. Linden, "Single Mode, Short Cavity, Pb-Salt Diode Lasers Operating in the 5, 10 and 30 μm Spectral Region", submitted to IEEE Journal of Quantum Electronics for publication in February, 1985 Special Issue